Technische Hochschule Ingolstadt

Mechanical Engineering

Renewable Energy Systems

Master's thesis

Subject: Comparison of different criteria for the grid integration of wind power

Name and Surname: Nikita Manonin

Issued on: 04.04.2023

Submitted on: 05.07.2023

First examiner: Navarro Gevers, Prof. Dr.-Ing. Daniel

Second examiner: Goldbrunner, Prof. Dr. Markus

Technische Hochschule Ingolstadt

Declaration

I hereby declare that this thesis is my own work, that I have not presented it elsewhere for examination purposes and that I have not used any sources or aids other than those stated. I have marked verbatim and indirect quotations as such.

Ingolstadt, 05.07.2023
(Date)

(Signature) 

Nikita Manonin

Abstract

The realization of the European Green Deal, remarkably increasing energy production from renewable sources, is in full swing. Some European countries have achieved high energy production performance, especially significant progress in electricity production from green technologies. A considerable share of renewable power comes from variable renewable sources, where wind power has a larger share, and fluctuating nature of which creates instability inside the electrical grid.

For these reasons, this master's thesis focused on issues of electrical grid stability caused by wind power penetration and the possibilities of determination of the maximum amount installed renewable power into a connection point.

The thesis contains the study of the dependence of electrical network stability on the number of several indices. The field of wind energy was considered in the first two chapters, represented by investigations of penetration level indexes and short circuit ratio.

So, an examination of the wind power penetration indexes is provided according to the main criteria: Rotor angle stability, Voltage stability and Frequency stability, the boundaries of which are set by system operator regulations. A simplified grid model with a share of wind power in MATLAB Simulink software for testing is designed with small and large disturbances. The short-circuit ratio section investigates the influence of changing short-circuit power and reactance and resistance ratio on grid parameters, implemented in a model of a grid-connected wind park in Simulink. The last chapter observes the simultaneity factor significance and influence under different renewable sources according to literature evidence and data analysis.

As a result, the work contains explanations, real examples and the influence degree of each coefficient on the grid stability. Also, limitations of installed capacity according to the index values are investigated. This work is helpful as a look at simplifying the formation of a commercial proposal based on additional criteria.

Table of Contents

Abstract iii

Nomenclature vi

List of Figures viii

List of Tables x

1. Introduction 1

1.1 Literature research 1

1.2 Scope of the Thesis 2

1.3 Thesis Outline 2

2. Initial provisions 4

2.1 Network design and existing connection regulations 4

2.2 Grid connection 6

2.3 Wind speed generation 8

3. Penetration level indices 11

3.1 Object of study 11

3.2 Existing values 13

3.3 Stability issues 17

3.4 Model 22

3.5 Wind power plant branch 23

3.6 Synchronous generator 27

3.7 Loads and additional equipment 29

3.8 Simulation and results 34

4. SCR 41

4.1 Grid strength 41

4.2 Model....42
4.3 Simulation and results....43
4.4 General influence....43
4.5 Searching for the limit....46
5. Simultaneity factor....49
5.1 General concepts....49
5.2 Influence on actual power....50
5.3 Results....53
6. Overall conclusion....54
7. List of references....56
8. Appendices....64
Appendix A....64
Appendix B....68
Appendix C....69
Appendix D....70
Appendix E....71
Appendix F....76
Appendix G....78
Appendix H....80
Appendix I....83

Nomenclature

List of abbreviations:

DGIF – Double-Fid Induction Generator

DSO – Distribution system operator

EN – European Norm

GS – Grid-side

MSWP – Maximum Share of Wind Power

PCC –Point of Common Coupling

PF – Power Factor

RS – Rotor-side

SCP – Short Circuit Power

SCR – Short Circuit Ratio

TRASI – Transient Rotor Angle Severity Index

TSO – Transmission system operator

WCP – Wind Capacity Penetration

WEP – Wind Power Penetration

WPP – Wind Power Plant

WT – Wind Turbine

X/R – Reactance to Resistance ratio

List of symbols:

P_n – Installed nominal power

P_{PC} – Capacity of primary control reserve

P_{SC} – Capacity of secondary control reserve

P_{TC} – Capacity of tertiary control reserve

D_n – Harmonic interference

E_{sc} – Impedance voltage of the transformer

I_{nl} – No-load current

I_{ref} – Turbulence intensity

L_{max} – Maximum anticipated load

P_{lt} – Flicker emission

P_{nl} – No-load losses

P_{sc} – Short-circuit losses

p.u. – per unit

η – Efficiency

C – DC bus capacitors

I – Current

L – inductance

R – resistance

S – Apparent power

V – Voltage

a – Phase shift

v – wind speed

δ – Rotor angle

σ – Standard deviation

List of Figures

Figure 1 Electricity production in the Europe Union 1

Figure 2 Electrical network diagram 4

Figure 3 Networks voltage levels in the United Kingdom 5

Figure 4 Schematic representation of general wind farm grid connection 6

Figure 5 Used connection types 7

Figure 6 Wind speed density. 10

Figure 7 Generated wind speed values. 10

Figure 8 Transfer capacity structure. 14

Figure 9 Indices annual values. 15

Figure 10 Indices monthly values. 15

Figure 11 Variable energy sources indices monthly values. 16

Figure 12 Additional characterizing parameters. 16

Figure 13 Usage of balancing energy. 17

Figure 14 Power system stability classification 18

Figure 15 Load angle curve 18

Figure 16 Model Diagram 1. 22

Figure 17 Schematic representation of a wind turbine 23

Figure 18 Wind turbine characteristic curve. 24

Figure 19 Wind speed test data. 26

Figure 20 Governor block 29

Figure 21 Electrical part of variable load 30

Figure 22 Calculation scheme of variable load 31

Figure 23 Power evaluation scheme of variable load 32

Figure 24 Day load profile 33

Figure 25 Consumption curve 33

Figure 26 Initial evaluation, large disturbance test 36

Figure 27 Frequency fluctuations in the limiting case 37

Figure 28 Model Diagram 2 43

Figure 29 Variable SCR, voltage values 44

Figure 30 Variable SCR, reactive power production 45

Figure 31 Maximum power value for small-signal case 47

Figure 32 Short-circuit test of turbine maximum power 47

Figure 33 Diversity factor for different number of generators 53

List of Tables

Table 1 Turbulence classes and turbulence intensities 8

Table 2 WEP indices examples 12

Table 3 Indices yearly values.....13

Table 4 Stability criteria summary 21

Table 5 Addition method 38

Table 6 Substitution method 39

Table 7 SCR testing levels.....44

Table 8 X/R calculated values 46

Table 9 French standard NFC14-100 49

Table 10 Simultaneity factor values in Germany 50

Table 11 Correlation values 51

Table 12 Various limit values of the simultaneity factor 52

1. Introduction

1.1 Literature research

One of the main parts of the European green deal is the clean energy transition, which is claimed that Europe Union should achieve carbon neutrality by 2050 (European Union, 2018). For this reason, the electricity produced from renewable sources is rapidly increasing, as shown in Figure 1.

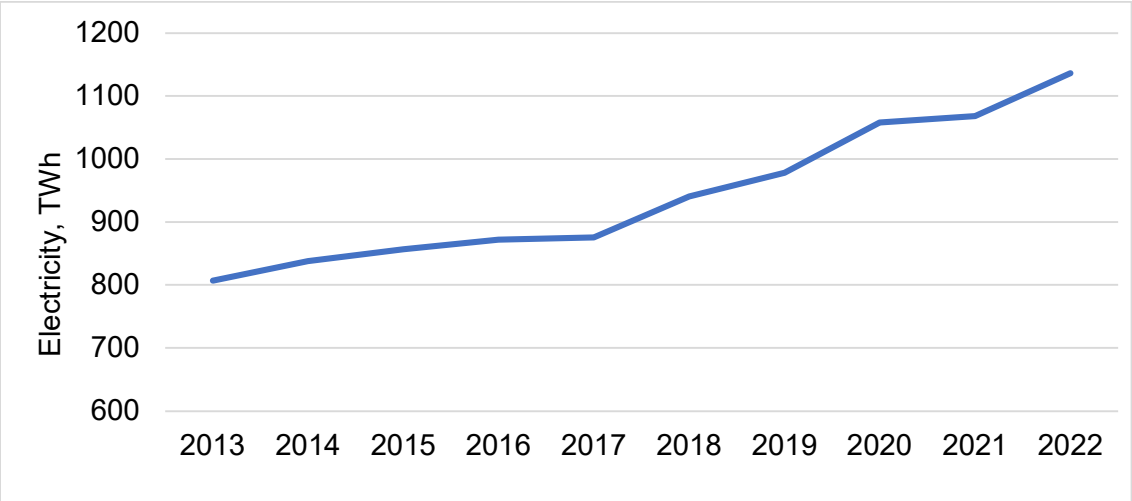

Figure 1 Electricity production in the Europe Union. Adapted from (IEA, 2022).

Nevertheless, 58% of this electricity is produced by a variable renewable source: solar and wind. Also, wind energy became more widespread compared to solar, which was 454,2 TWh versus 206,2 TWh, respectively, in 2022 (IEA, 2022). Moreover, this is a severe challenge for grid stability.

The electricity production from renewable sources fluctuates, but fluctuations in small capacity quantities are not an issue for system stability (Earnest, 2019). However, the power increase from the sources leads to colossal variability and unbalance between supply and demand in a system. There are many kinds of interactions with this problem, such as increasing requirement reserve power (Impram et al., 2020), development of a Virtual power plant concept (Liu et al., 2023) and many others. But it is undoubtedly more convenient to initially determine the maximum limit of the oscillating renewable energy in the system as a whole or in a particular part of it. In turn, there are also many approaches to solving this problem. Researchers of this problem allow one to go deep into different theoretical and practical methods. It can be a definition of the minimum Short Circuit Ratio (SCR) for a grid (Reginatto and Rocha, 2009) or an investigation of a Voltage stability margin (Lei et al., 2022). In general, the definition of an index is a convenient approach for a customer and designer to quickly estimate the amount of renewable power that can be installed on the grid.

1.2 Scope of the Thesis

So, the research objectives are using indices to determine the degree of stability of the system, particularly the limits of renewable capacity that can be connected to the network at connection points.

Mainly, the focus is on wind energy and related indicators, where Germany as a region was selected for both wind data and technical interconnection regulations.

The indexes are divided into three groups:

- Wind Capacity Penetration (WCP),
  Wind Energy Penetration (WEP),
  Maximum Share of Wind Power (MSWP).
- SCR.
- Simultaneity Factor (SF).

The main goal of the work for the two first groups is implemented by creating a model in MATLAB Simulink. Additionally, indexes from the first and third groups are investigated using German electricity market data. Also, the penetration-related indices and the Short-Circuit index are considered in the context of wind energy, while the last one is studied for more common renewable energy sources in the selected region.

1.3 Thesis Outline

As was described before, the master's thesis is divided into three main sections, which are contained in Chapters 3,4 and 5. The initial positions used throughout the work are shown in the 2nd chapter, and the overall conclusion is in the 6th section.

The 2nd section defines used terms, provisions and data for future modelling. The chapter begins with discussing the topic of typical grid organization and possible connection regulations for generators. The next step is to introduce a scheme of grid connection, and at the end is a description of a wind speed generation program.

The 3rd chapter is about two penetration indexes and a limitation index. Demonstrated actual values are shown for the selected region and process of creation and testing of a simplified grid model with a wind power plant under different penetration levels. The final part contains the processing of obtained data and corresponding conclusions.

The 4th chapter is about the SCR index. Also, the chapter contains an investigation of the reactance and resistance ratio, which is linked to the SCR. The chapter starts with initial definitions and a description of a grid-connected wind plant test model. The

following section is about the stability tests. This chapter ends with results and conclusions.

The 5th chapter talks about the SF index. It contains a definition and implementation of the SF index from the supply and production sides. Further is going a demonstration of the possible impact on the index and its relationship with installed capacity.

Finally, the last chapter consists of the overall conclusion and results of the whole work.

Appendix A contains the grid code by the European Association of Transmission System Operators.

Appendix B contains the program in R language for wind speed generation data.

Appendix C contains the 1st section indexes calculated in monthly dimensions.

Appendix D demonstrates time-voltage limits from chosen grid code during and after short-circuit fault.

Appendix E includes the wind turbine's block controlling diagrams, exemplary parameters, and transformer parameters for the calculation. Also, the accessory load and transformer, which are related to the wind farm branch, parameters are shown.

Appendix F shows control schemes and parameters for a synchronous generator and its auxiliary equipment.

Appendix G contains the parameters of load blocks and derivations of equations, which describes the works principle of custom load block.

Appendix H contains the calculation results of the penetration indexes chapter.

Appendix I shows 3-phase source block parameters and voltage diagram during the fault for the accepted minimum value of SCR.

2. Initial provisions

The chapter addresses initial definitions, data and methods for modelling and implementation in further chapters. Initially, a description of a typical network and example of a grid code are represented. Further, the main points of a WPP connection are explained. Finally, this chapter contains an explanation and program for generating Wind speed, which is also used inside the models.

2.1 Network design and existing connection regulations

For the investigation of thesis questions, it is necessary to denote major points of work mechanism and related constraints of common grids. The simplified scheme of the electrical grid is shown in Figure 2.

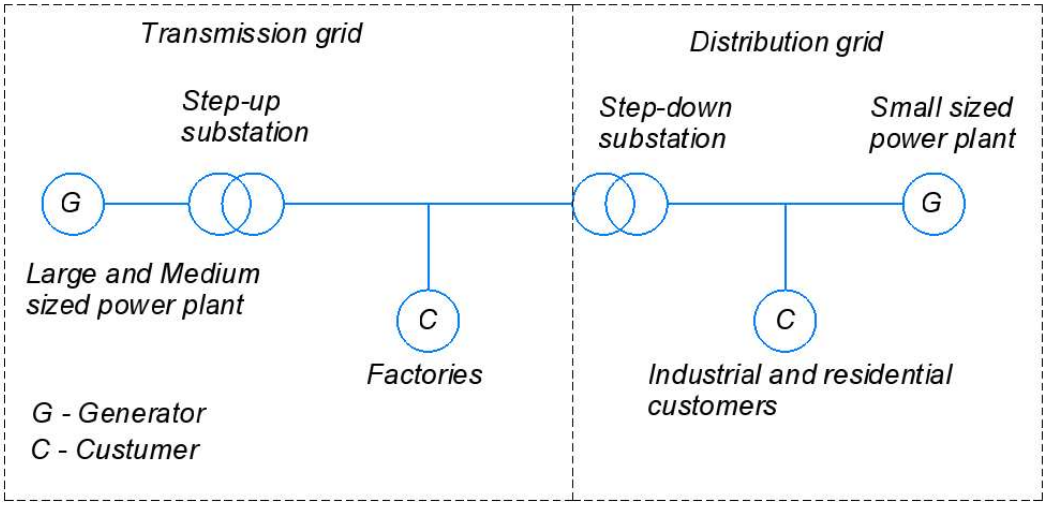

Figure 2 Electrical network diagram. Adapted from (Earnest, 2019).

So, according to the source (Earnest, 2019), a common grid consists of 2 main parts: Transmission and Distribution parts, and 2 types of participants: Generators and Consumers. Where Generation and Consumption are commonly separate private entities, which connect to Transmission or Distribution lines and must comply with codes for both connection and operation. Connection selection simply depends on profitability and capacity: the more power to be connected, the higher the voltage level should be chosen in order not to lose much energy when transmitting or receiving (Earnest, 2019).

Wind power plants are no exception and can be connected to both Transmission and Distribution lines, that is, to medium or high voltage levels (Earnest, 2019). The correspondence between the voltage levels and the part of the network is shown in Figure 3. However, these ranges depend on the country considered. For example, in

Germany, low-voltage level represents a voltage up to 6kV, medium voltage from 6kV to 60kV and high-voltage levels from 60 kV to 220 kV (BMWK, 2023).

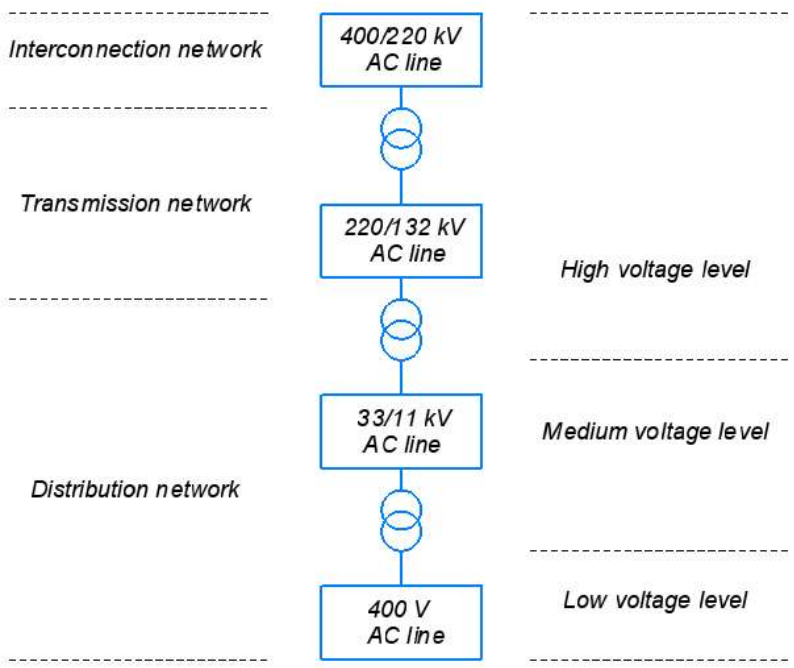

Figure 3 Networks voltage levels in the United Kingdom. Adapted from (Earnest, 2019).

Distribution and Transmission networks contain power lines and auxiliary equipment based on different voltage levels, which belong to various private firms, named operators, whose main goals are stability maintenance and operation on their parts of the networks (Earnest, 2019). In particular, Transmission System Operators (TSO) are responsible for the balance of the entire system. Due to it, TSOs and Distribution System Operators (DSO) participate in regulation forming. There are many different regulation levels, such as international, national, regional and other additional commissions, which are also responsible for recommendations and adoption of standards (Ackermann, 2005). Thus, despite the similarity in the main points, depending on the region and company, some issues may differ, for example, the time before disconnection in case of overvoltage (Ackermann, 2005).

According to the objectives of the work, this chapter considers regulations for grid-connected generators, named Grid Code, which contains operational rules and possible limits. An example of a grid code main points for connection in the high voltage level of transmission lines under authorities of German company „E.ON Netz” (at the moment, these transmission lines belong to the „TanneT” company) and these regulations are shown in Appendix A.

The requirements related to generators can be divided according to observed parameters: Active power, Reactive power, Frequency and Voltage (Ackermann, 2005). Each of them has frames for fluctuation in the stable state, where the value must be

within 95% of observation time and time to return to the required range in case of exit from it. Also, each set value applies to different time values. For example, Active power should be measured as a 1-minute average, and frequency is compared as a 10-minute average and so on. In addition to boundaries, qualitative values such as flicker, harmonics and rapid changes are also determined for voltage. Finally, the list of requirements includes the rules during startups, shutdowns and faults. These statements above are taken from the source (ENTSO-E, 2013).

So, these requirements commonly represent the finalization of several standards, such as (IEC, 2001) from the International Electrical Commission, “Requirements for Grid Connection” by ENTSO-E, which is an association of European Transmission Operators, and company “E.ON Netz”, which provides these requirements directly to their customers (Ackermann, 2005).

2.2 Grid connection

As was mentioned below, wind power can be connected to a grid at different voltages level, so necessary designate the connection scheme and connection point, namely the Point of Common Coupling (PCC). The PCC is the point of separation between the network and the wind farm, often located near the measuring device (Clausen, 2013). The above network requirements apply to the measurements at PCC. The wind park's connection to a high voltage level of a grid is shown in Figure 4.

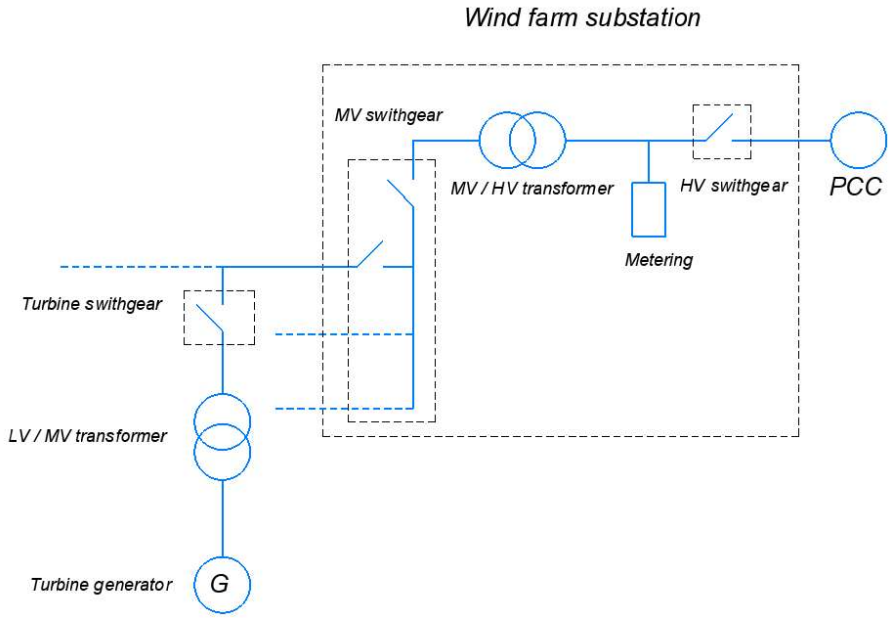

Figure 4 Schematic representation of general wind farm grid connection. Adapted from (Clausen, 2013).

According to the source (Clausen, 2013), the standard equipment set for connection includes:

- Low-voltage level: turbines, low-medium voltage step-up transformers, generally located at the bases of turbines, and switchgear for each turbine.
- Medium-voltage level: medium voltage cables, connected turbines and the main farm transformer, switchgear on the wind farm side and medium–high (or medium–medium) voltage transformer.
- High-voltage level: switchgear, measuring device and high voltage lines.

In general, onshore WPPs are connected to the Distribution level because most wind plants are in rural areas and offshore to the Transmission network due to their power size (Earnest, 2019).

The process of choosing the connection type is complicated enough and depends on several factors. First of all, the connection type depends on the grid parameters, such as Short Circuit Power (SCP), which demonstrates the overall strength of the grid. This parameter is discussed further. Also, serious effects are going from the length of necessary connection cables and, as said, installed power of the plant (Clausen, 2013). For example, Direct Current (DC) is preferable for long-distance transmission to Alternating Current (AC) because DC lines have lower losses than AC lines, and PF correction should be used for AC lines due to the cable's capacitance (Clausen, 2013). However, using DC is more expensive. Additionally, if higher voltage, the losses are lower, but the cost of such cables is more costly (Clausen, 2013).

So, there are several common types of offshore wind plant connection (Clausen, 2013): High Voltage Direct Current (HVDC), Medium Voltage Alternating Current (MVAC) and High Voltage Alternating Current (HVAC). The application is shown in Figure 5.

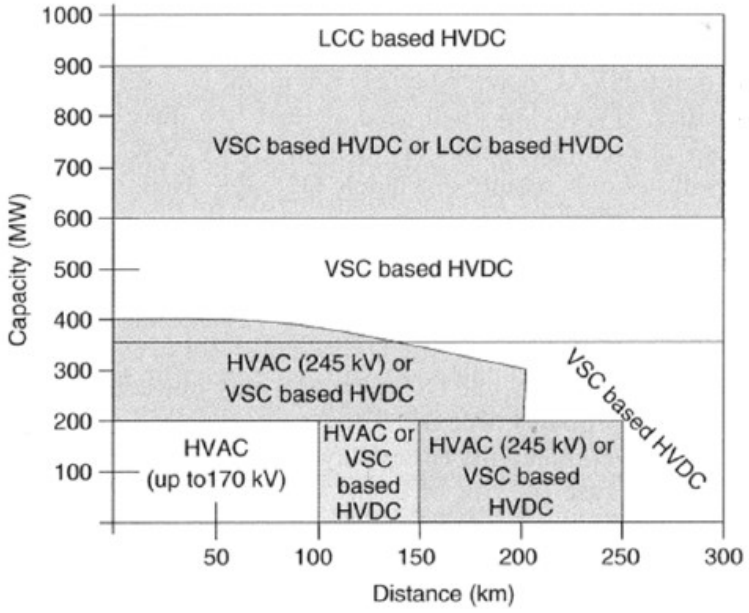

Figure 5 Used connection types (Clausen, 2013).

Where VSC is the voltage source converter, and LCC is the commutated line converter.

Furthermore, the most popular onshore is MVAC (Earnest, 2019). As shown below, to simplify as much as possible, the wind farm interconnection consists of a turbine and one generator, which combines the functions of the two presented above.

2.3 Wind speed generation

The initial provisions are necessary for understanding the problem that have been described in the previous subchapters. This section is also devoted to one of the important starting parts of this paper - wind speed modelling. Generated wind speed has used in the Simulink models.

The variable nature of wind speed is the main the issue of grid stability. So, the main factor of wind speed fluctuation is turbulence, defined as “wind fluctuations with periods less than the averaging period” (DNV GL, n.d.). According to the standard (IEC, 2005), the wind speed follows the Weibull distribution. Also, the standard provides a formula for relationships between mean wind speed and standard deviation coefficients as shown in Equation 1.

$$\sigma = I_{ref} * (0{,}75 * v + 5{,}6) \quad (1)$$

Where σ is a 10 min. wind speed standard deviation, I_{ref} is turbulence intensity, and v is 10 min. mean wind speed (IEC, 2005). The value 5,6 chosen as a constant for rotors bigger than 50 m in diameter (Hannesdottir et al., 2018). The turbulence intensity value depends on turbulence classes, this correspondence is shown in Table 1.

Table 1 Turbulence classes and turbulence intensities (IEC, 2005).

Turbulence classes	I_{ref}
A	0,16
B	0,14
C	0,12

Nevertheless, providing data for each second for correct simulation is necessary. For this reason, was created a program in RStudio, with the following central ideas:

1. Creating 10 min. data of mean wind speed based on the first artificially accepted mean wind speed value and standard deviation parameters for Weibull distribution.
2. Development another Weibull distribution, for 1-sec wind speed data, is located "inside" the previous.

These data are calculated as a Weibull distribution function with the following parameters:

- Mean wind speed value corresponding to the given interval.
- Furthermore, standard deviation values should be evaluated by Formula 1 for 10-minute values and assumed fixed value for 1-sec values for simplification.

The result is fluctuating wind speed data for each second and Weibull distributed. The program is attached in Appendix B, and its mechanism is described further.

So, the mean wind speed equals 6,77 m/s, as an average wind speed at 100m high in Germany for 2022 (Global Wind Atlas 3.0, 2023), and Turbulence classes A, as the case of most significant fluctuations, both are accepted as initial data. Further, a cycle for the generation of the wind turbine speed was created for the necessary duration (1200 seconds in this case) with the possibility of setting mean wind speed for 10-minute intervals:

1. Calculation of standard deviation, taking the German average wind speed as the initial value for mean wind speed, according to Formula 1
2. Conversion of the values of the normal distribution and the average speed to the shape and scale by specific function for generating 1st Weibull distributed value of mean wind speed (this is 10 minutes average values create first array)
3. Adoption of another standard deviation, in particular for the seconds' values (it was taken as the square root of 4,5 because, after calculation, this value is slightly more than the maximum standard deviation calculated for 10-minute series)
4. Repeating step 2 by taking the last calculated mean wind speed and standard deviation from step 3 and generating 600 values (data for inner second array)
5. Accepting the 601st value as the new initial average speed (next value from the first massive) and repetitions according to the required total duration

Additionally, it is possible to set unrelated average 10-minute values if 600 seconds is enough to test a particular state, and it is necessary to try several different conditions. The result shows distribution of generated values is shown in Figure 6.

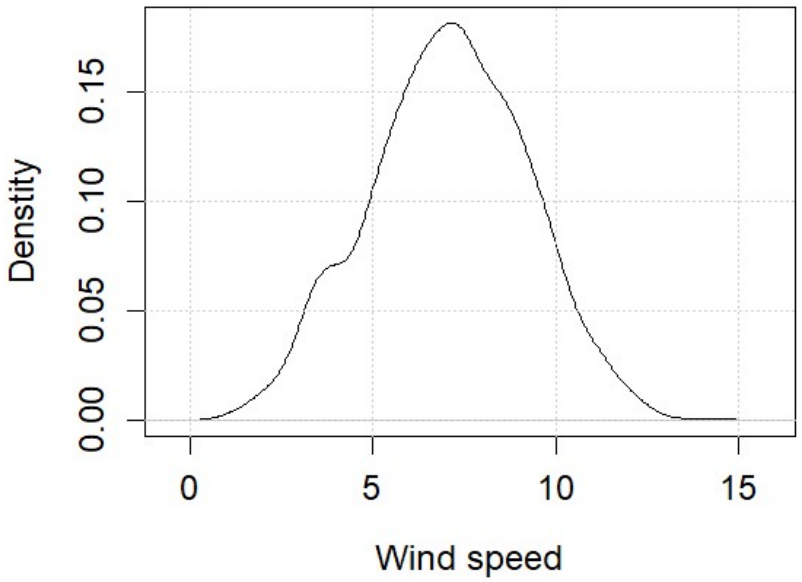

Figure 6 Wind speed density.

An example of the program is placed in Appendix B. The generated value for each second is shown in Figure 7.

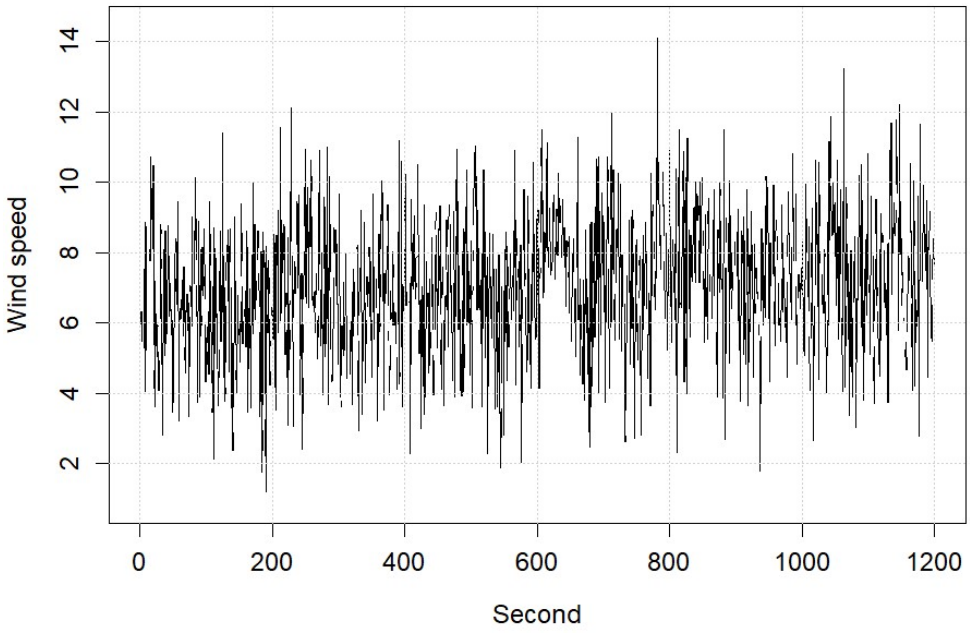

Figure 7 Generated wind speed values.

It is necessary to emphasize that, in general, the shape parameter is correlated with the wind climate of the location and should preferably be defined in another way (Navarro, 2021b). But this is one of the simplifications, and it is necessary to choose the mean wind speed directly.

3. Penetration level indices

This chapter is dedicated to observing indexes related to wind penetration into a grid and one restrictive index. Definitions and evaluation methods of the indexes are presented at the start of this chapter. Examples of indices calculated based on the German energy market are also given. In the end, this chapter explains the research model, obtained results and conclusions based on considered questions.

3.1 Object of study

The influence size from wind power to a grid operation depends on the network parameters, such as generation mix, the grid size and strength, and the wind power penetration (Earnest, 2019). The grid size can be represented as off-grid systems or regional or national networks, and the less energy is produced and consumed, the easier and less it is necessary to control the grid. The grid strength evaluates operational conditions and the possibility of the system staying stable following a disturbance (Golieva, 2015). The Generation mix in a power system combines different fossil and renewable electricity generation sources. Each of these parameters defines and influences stability, thereby determining the possible value of the connection of variable energy sources (in the PCC or the entire network) from the side of the network itself (Ackermann, 2005). So, this chapter highlights the problem from the side of introducing wind energy. Hence the chapter focuses on the research of penetration and limitation indices.

Following considered indices, represented in the source (Earnest, 2019):

The Wind Capacity Penetration (WCP) is an instantaneous value expressed as a percentage that equals the Installed wind power capacity divided by the peak load in MW units. The WCP evaluates the amount of peak load that can be theoretically covered by wind power in a particular region over time. This index is demonstrated in Equation 2.

$$\mathrm{WCP}\ (\%) = \frac{\text{Installed wind power capacity (MW)}}{\text{Peak load (MW)}} * 100 \quad (2)$$

Since it is an instantaneous value, it is more related to the stability in the short-term value, such as during a fault and Transient stability, which is discussed below. This index is enough convenient value for using as limitation criteria of wind capacity installation because it considers capacities directly calculated or indicated in technical data sheets.

The next index is Wind Energy Penetration (WEP) equals the relation between the Annual production of wind energy and Gross annual electricity demand, both in TWh,

expressed in percentage and a region for commonly a yearly period. The index is presented in Equation 3.

$$\text{WEP}\ (\%) = \frac{\text{Annual production of wind energy (TWh)}}{\text{Gross annual electricity demand (TWh)}} * 100 \quad (3)$$

The criterion demonstrates the amount of energy demand covered by wind energy, in particular a supply and demand balance for a long-term period. This means that it refers closer to small disturbances stability testing. So, the index is easy to estimate and can act as a limiter for establishing wind power at the system connection point based on annual data. Examples of existing values of the WEP index are represented in Table 2.

Table 2 WEP indices examples. Adopted from (Ackermann, 2005).

Region	WEP (%)
Navarra (Spain)	50
Schleswig Holstein (Germany)	28
Crete (Greek)	10

The last observed in this chapter index is the Maximum Share of Wind Power (MSWP), which represents the upper limit of possible wind-generated power. MSWP is the percentage value, represented as the Maximum generated wind power in MW, divided by the sum of minimum load and power exchange capacity with other regions in MW. The index is shown in Equation 4.

$$\text{MSWP}\ (\%) = \frac{\text{Maximum wind power generated (MW)}}{\text{Minimum load (MW)} + \text{Power exchange capacity (MW)}} * 100 \quad (4)$$

This auxiliary index also allows one to determine the maximum possible penetration level. The minimum load, particularly a base level, can constantly compensate for wind power production. Also, the exchange capacity consumes some amount of electricity. So, this index is based on the supply-demand balance and demonstrates the limit after which electricity from wind energy have to be wasted to save the stability regime of a grid. Thus, the index indicates the balance in a system when remaining below 100%. If MSWP approaches or exceeds 100%, it signals the need to reduce wind power production in the region or increase transfer capacity. This criterion correlates with network bandwidth and reveals problematic areas, which may introduce an imbalance due to electricity excess. Also, it is highly dependent on chosen area scale and time frames because instantaneous values are used. All these criteria are discussed in this chapter.

3.2 Existing values

For the indexes evaluation and other related parameters on a real example used, open data of the German electricity market was provided by (SMARD, 2023). The data with a time resolution of 15 min and 1 hour, depending on data type, and with a time frame from 01.01.2015 to 31.08.2022 for entire Germany was observed. The following data types were considered:

- Actual generation. This data consists of the electricity produced in MWh for each 15-minute. The represented source types: Nuclear, Biomass, Wind onshore, Photovoltaics, Lignite, Hard coal, Fossil gas, Hydro pumped storage, Hydropower, Other renewable, Other conventional, and Wind offshore.
- Installed generated capacity. This is the installed capacity in MW for each type of power source listed previously. The data is represented for each hour. However, in reality, they are updated annually at year start.
- Actual consumption. These are the average value of the sum grid load for 15-minute intervals in MWh.
- Exchanges. This data type represents the amount of electricity in cross-border flows between countries. Net export and net import for Germany in units of MWh are included. The time resolution is at 15-minute intervals.
- Balancing energy. Balancing energy, used to maintain stability in the region, is divided into electricity volumes in times of shortage and surplus electricity. Both categories are in MWh and have a 15-minute resolution.

According to the data, it is possible to evaluate the indexes for year and month dimensions. 15-minute resolution is used because it allows one to assess instantaneous or limitation values more accurately. The calculation of WEP, WCP and MSWP are made according to Formulas 3,4 and 5, respectively, annually and monthly. Table 3 demonstrates the yearly values.

Table 3 Indices yearly values.

Year	2015	2016	2017	2018	2019	2020	2021	2022
WEP, %	15,43	15,39	20,29	21,28	24,99	26,78	22,48	25,91
WCP, %	49,92	56,06	64,44	70,91	76,96	77,40	76,81	80,17
MSWP, %	53,31	57,34	63,70	71,14	79,38	80,74	70,71	76,96

As mentioned earlier, 2022 is considered until August 31 inclusive. Instantaneous values, such as peak loads for WCP, minimum load and maximum generated wind power for

MSWP, were accepted according to the data with 15-minute resolution. That is, the smallest or the most considerable 15-minute average value for the corresponding period. Also, the exchange capacity is accepted as the value used in cross-border flows, which is a smaller value compared to the power exchange capacity and, as a result, artificially increases the value of the index. An overview of a transfer capacity structure is shown in Figure 8.

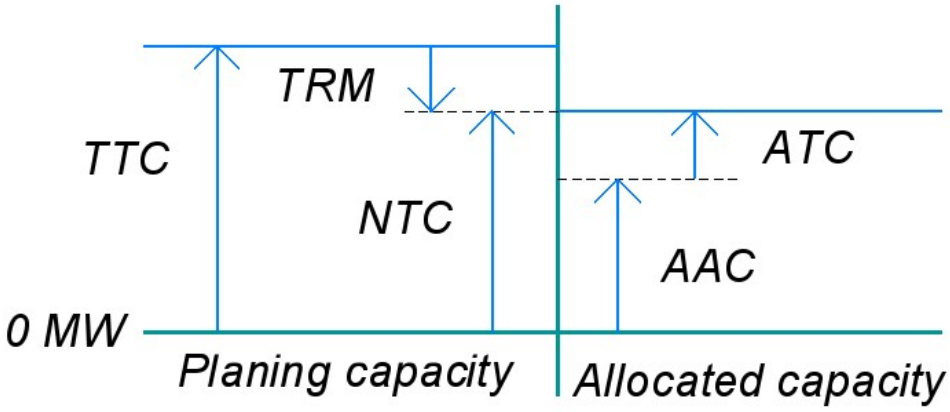

Figure 8 Transfer capacity structure. Adopted from (European Transmission System Operators, 2001).

So, the Total Transfer Capacity (TTC) includes the Transfer Reliability Margin (TRM) and Net Transfer Capacity (NTC), which is the limit for the subsequent transmission of electricity (European Transmission System Operators, 2001). These values are calculated iteratively by the regulator based on previous data (Amprion GmbH, 2015). So, the required value for power exchange capacity equals NTC. However, this data type is incomplete and contains many missing values (ENTSO-E, 2023). Therefore, it was decided to use data from transboundary flows, which tend to the NTC value.

The allocation of transfer capacity is equal to NTC and consists of Available Transmission Capacity (ATC) and Already Allocated Capacity (AAC) (European Transmission System Operators, 2001). AAC is known in advance and fully included in the accepted value. ATS is the remaining capacity after allocation and commonly particularly counts in the taking value of cross-border flows (European Transmission System Operators, 2001). Thus, the calculated values of MSWP are not very accurate.

Thus, Figure 9 and Figure 10 show the calculated indexes for annual and monthly periods, respectively, to consider the influence of the chosen time scale.

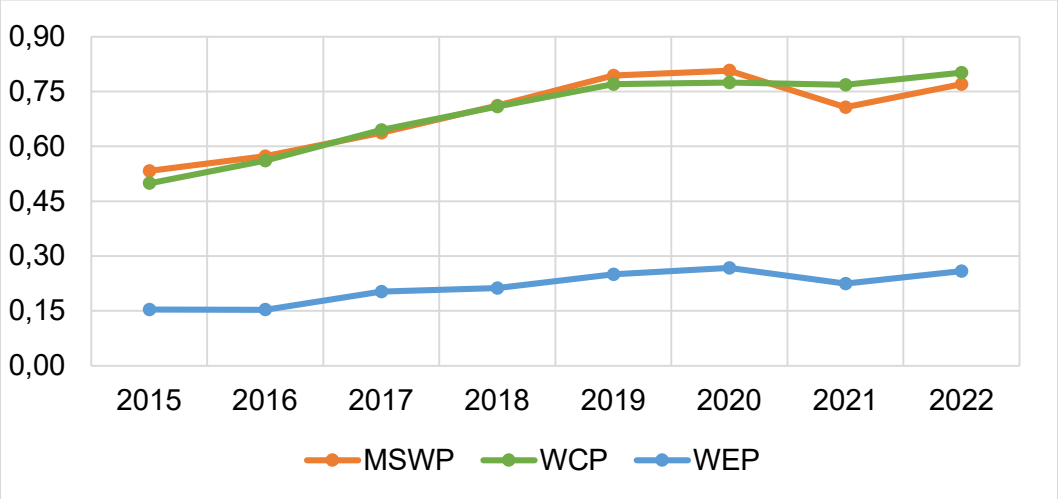

Figure 9 Indices annual values.

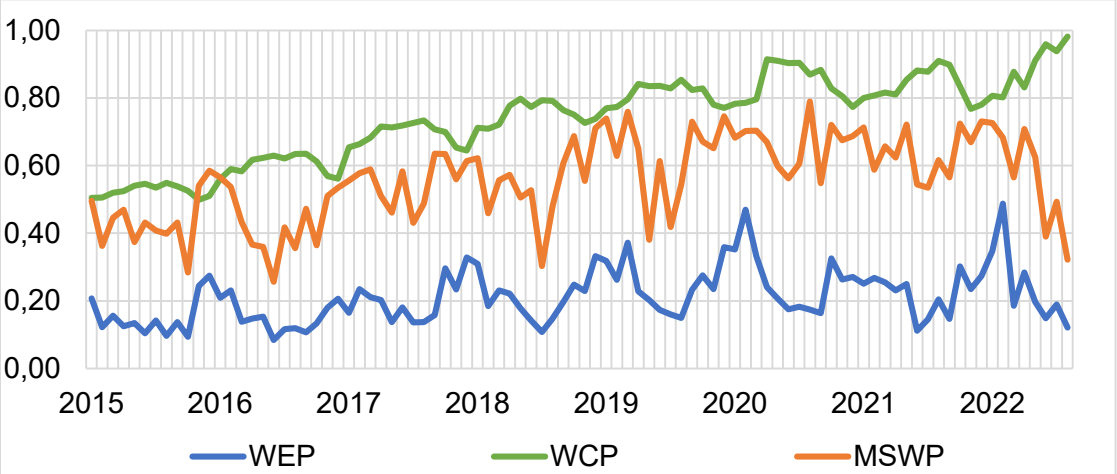

Figure 10 Indices monthly values.

It is seen that the monthly calculated indexes are subject to fluctuations due to the season. For MSWP, the reduction of the observation scale is unacceptable, since the task of evaluating a critical case, according to observations, occurs in the winter seasons, and limiting values are contained with yearly scale figures. The same negative effect is on the WCP, where a yearly graph display only the minimum annual values of the monthly chart. For WEP, a larger time scale smoothes the picture, which on the one hand, yearly data is helpful due to deleting the influence from the seasons. On the other hand, the monthly index displays the situation in more detail. This correlates with base definitions that MSWP and WCP are instantaneous values. Hence, a downscale of time resolution is necessary for them, but for WEP, it works conversely.

Since solar energy is also developed in Germany and is warm energy, it is possible to evaluate these indices of all variable renewable energy and compare them with the situation in the region. These parameters are represented in Figure 11.

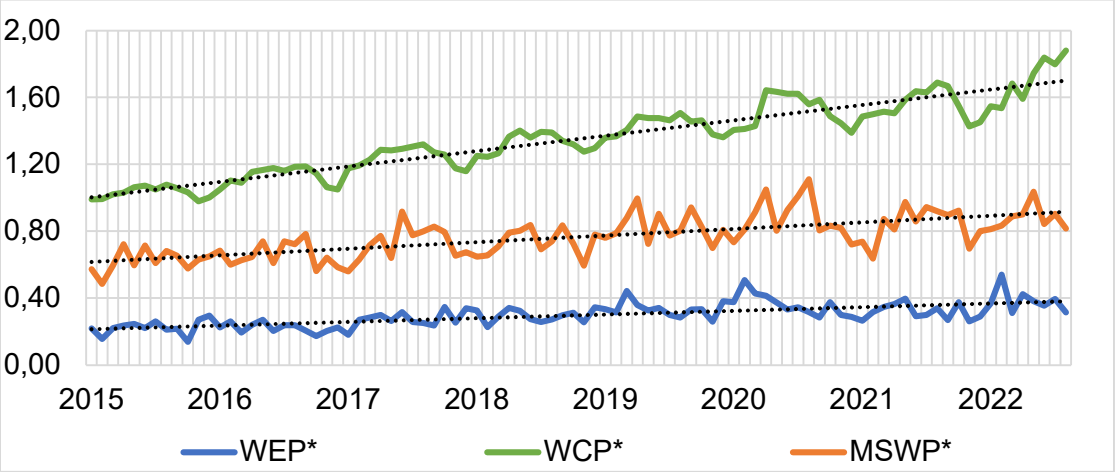

Figure 11 Variable energy sources indices monthly values.

This graph additionally contains linear trend lines. Also, previous comments remained.

For completeness, the picture in Figure 12 shows additional parameters such as overall produced electricity from variable sources, total consumption, and usable transfer capacity for a rough estimate of the situation in the region. Figure 13 contains the amount of average balancing energy in one h. The yearly data are represented in Appendix C.

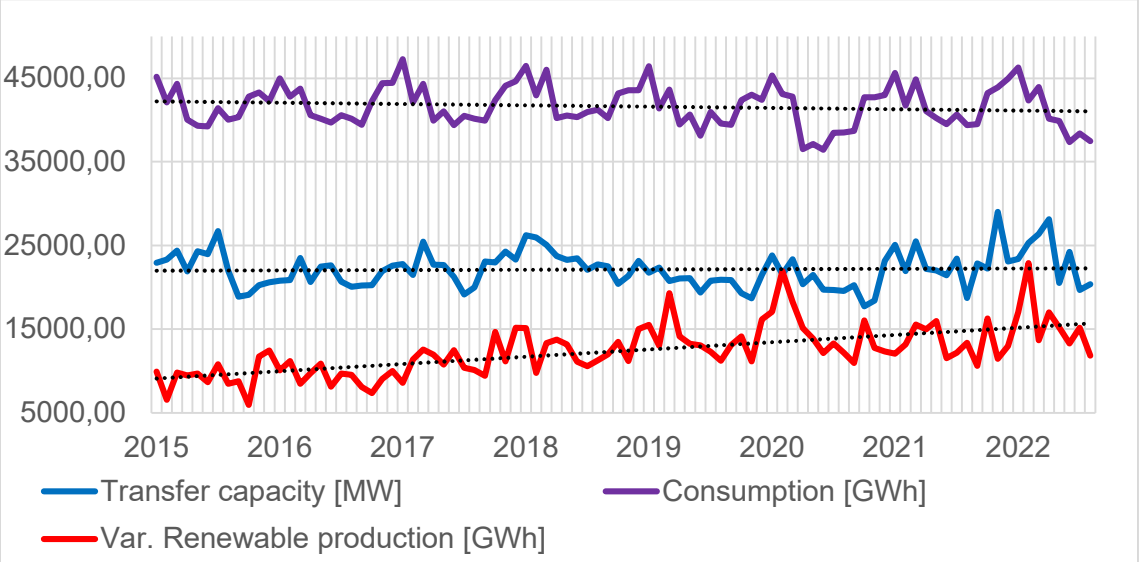

Figure 12 Additional characterizing parameters.

The left axis represents values for consumption and production, and the right axis represents figures for balancing. The graphs contain linear trend lines.

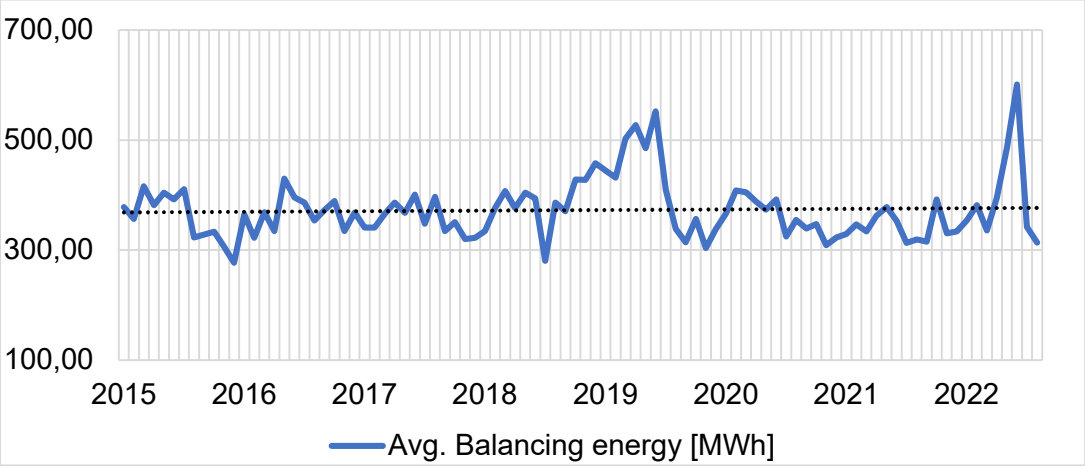

Figure 13 Usage of balancing energy.

It should be noted that, during the observation period, electricity consumption has tiny decreased, and the share of variable energy has increased. All this corresponds to the motion of WCP* and WEP* indexes. Also, the value of the transferred capacity is approximately constant, and the MSWP* index grows slightly throughout the observed period. However, the overall trend in the use of balancing energy remained at the same level, except for excesses due to the start of covid restrictions in 2019 and Europe's energy crisis in the first quarter of 2022. While the amount of usage balancing energy is one of the indicators of grid stability (SMARD, 2021). So, despite the increase in the penetration level of variable renewable sources into the network, the parameter associated with the system's strength remains constant. Unfortunately, this observation does not allow for the making of any conclusions because there are vast amounts of different factors that cannot be taken into account within the available data and affect the usage of balancing energy. For a more detailed and justified conclusion, it is necessary to provide a more thorough analysis based on modelling and deep into stability issues.

3.3 Stability issues

The system stability analysis is divided into the following categories: frequency, voltage, and rotor angle, which also are divided depending on the size and duration of the disturbances (Yadav and Saravanan, 2022). Large disturbances are commonly caused by short-circuit faults (IEEE, 2020). Small disturbances are typically set using ramp signals since for a small signal the parameters of the system change almost linearly, and linearization of the equations around the equilibrium point is possible (IEEE, 2020). So, for the system is possible to use consumption changes in a ramp form to implement small disturbances (Swe, 2020) or sharp changes in power production, which simulates possible temporary wind plant shutdowns (Sajadi et al., 2019). Three of these signals are implemented in this work. The structure of stability analysis is demonstrated in Figure 14.

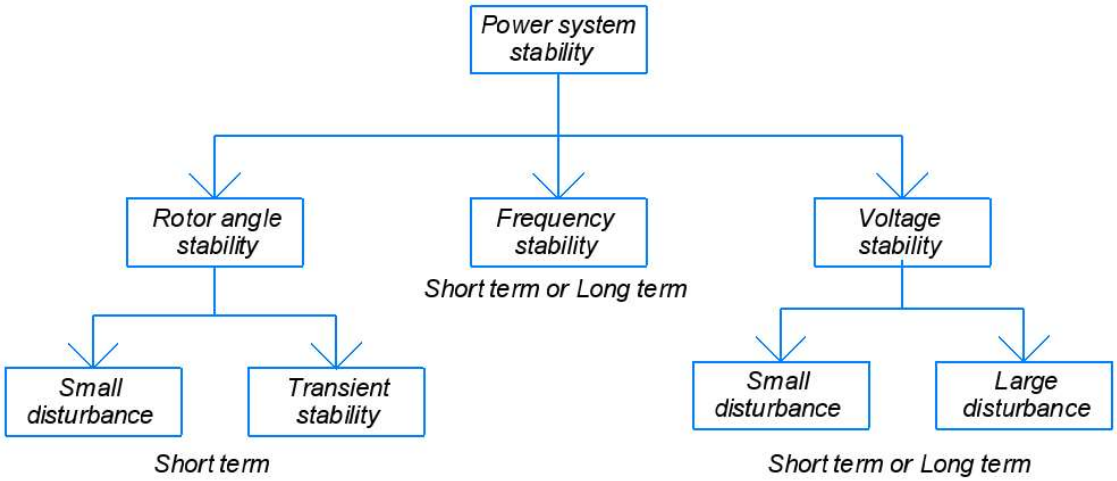

Figure 14 Power system stability classification. Adapted from (Yadav and Saravanan, 2022).

In the beginning, the rotor angle stability is considered. It is known that there is a large amount of generation equipment in a system, for instance, diesel generators, which use a synchronous machine for electricity generation. System synchronisation problems, mainly expressed by rotor angle issues, can be observed by large and small short-term disturbances (Toma et al., 2021).

The angle between a stator and rotor magnetic fields of a synchronous machine, named internal angle or rotor angle, defines electrical power output, stability region and mode of operation (Earnest, 2019). So, the part of the Generator mode is up to 180 degrees, and the stable condition is up to 90 degrees (Lackovic, 2023). These points are shown in Figure 15.

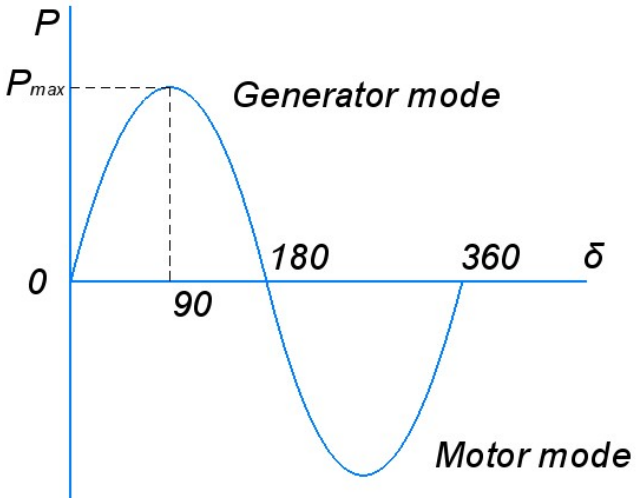

Figure 15 Load angle curve. Adapted from (Lackovic, 2023).

In systems containing several synchronous machines where stationary mode is violated, the angles of the rotors of the machines differ. This difference is named relative rotor angle and demonstrates the link between rotor angle and system stability (Lackovic,

2023). Thus, the rotor angle should be less than 90 degrees for small system disturbances.

During the large disturbance (transient stability), the rotor angle can go far beyond the boundaries of stability defined earlier but, at the same time, return to a stable state, and, in this case, the stable limit of the rotor angle is 180 degrees (Lackovic, 2023). It is also significant to emphasize that achievement and excess of stability limit do not guarantee that a machine becomes unstable (Lackovic, 2023). The generators tend to become unstable, and seriously exceeding the limit increases the chances of becoming unstable.

For a more accurate definition of a system stability level, according to rotor angle criteria, is used a Transient Rotor Angle Severity Index (TRASI) described in the source (Meegahapola and Flynn, 2010). Where TRASI closer to 1 indicates a stable system, and closer to 0 is an unstable system.

The TRASI index is shown in Equation 5.

$$\text{TRASI} = \frac{360 - \max\left(\delta_{max}^{pst}\right)}{360 - \max\left(\delta_{max}^{pre}\right)} \quad (5)$$

Where δ_{max}^{pst} is a maximum value of rotor angle after disturbance and δ_{max}^{pre} – before disturbance, the 360 degrees is used as a more significant value than the 180 degrees limit of a stable state and as the „maximum" possible angle which can be reached in an unstable state (Meegahapola and Flynn, 2010). A comparison between rotor angle values can be provided in small disturbances by evaluating the maximum angle during the observation period.

The next object for observation is Frequency stability. The main regulation frames define the upper and lower values of the regular operation regime. The main reason for instability in frequency is an imbalance between supply and demand. Also, it occurs due to fluctuations of wind and load in a network with wind energy penetration.

Differences between this parameter's long-term and short-term stability depend on the possible response, particularly on the volume of reserves and the speed of their application. There are three different levels of reserve powers for balancing a system (Milligan et al., 2010):

- Primary control reserves,
- Secondary control reserves,
- Tertiary control reserves.

Each stage provides the particular duration for maintaining the balance of supply and demand. According to chosen region, the recommended reserves capacities for a system are defined in equations 7 – 9 respectively (Milligan et al., 2010):

$$P_{PC} = 0{,}02 * P_n \quad (7)$$

$$P_{SC} = \sqrt{(a * L_{max} + b^2 - b} \quad (8)$$

$$P_{TC} = \text{Largest installed generation capacity} - P_{SC} \quad (9)$$

Where P_n – installed nominal power, L_{max} - maximum anticipated load for the control area [MW], a and b – constants, which equal 10 MW and 150 MW accordingly. Also, for the reserve, various sources of electricity are necessarily used (Milligan et al., 2010).

The last part of the stability analysis is Voltage stability. Commonly, voltage instability occurs due to the inability of the system to satisfy the demand for reactive power in different parts (Earnest, 2019). So, the source (Londero et al., 2015) considers several types of wind turbine control with the implementation of additional equipment to investigate this issue. However, looking ahead, a simplification approach used in this paper does not allow deep into this question. Thus, reactive power regulation nearby wind parks can be achieved using PF restrictions, as described in Chapter 2. Also, there are two main categories of voltage regulations: limiting ranges and voltage quality (Londero et al., 2015). Due to the specific work and complexity of voltage quality evaluation, in particular flicker and harmonics values, in the model, the required operational ranges have been used as the primary regulation with the outer limits according to the duration for minor disturbances. Also, of course, the reactive power regulations are considered.

For this case, the most common voltage problems in electrical networks, such as short-term large voltage disturbance, represented by the short-circuit fault, and long-term small voltage disturbance caused by gradual load changing (Hatziargyriou et al., 2021), are considered. Additionally, the scheme contains short-term small voltage disturbance, which is implemented by wind power fluctuation and is a widespread problem (Chouket and Krichen, 2015). The Long-term large voltage disturbance is not included in the tests because a common cause is the shutdown of equipment, which is not possible for the accepted model, which is shown later (Hatziargyriou et al., 2021).

To avoid complicating the scheme, the model contains a connection of wind power on the medium voltage level. So, the regulations for the interconnection are different compared to high voltage connection, described in Chapter 2. In this case, a grid code

has chosen according to a German Association of Energy and Water Industries „BDEW", described in the sources (BDEW, 2008). So, Table 4 summarises the requirements the model must comply with and the research methods for each point of stability tests.

Table 4 Stability criteria summary. Adopted from the source (BDEW, 2008).

Case of stability analysis	Frames and additional observed indexes
Rotor angle stability: Small disturbance	Rotor angle ≤ 90.
Rotor angle stability: Transient stability	Rotor angle ≤ 180, TRASI ≤ 1.
Frequency stability	Frequency normal fluctuations range from 47,5 Hz ... 51,5 Hz. In case of leaving from range, the source should be disconnected after 100 ms.
Voltage stability: Small disturbance	Voltage general time limited fluctuations limits: 80% ... 108% of nominal voltage with disconnection time 1,5 and 60 seconds respectively; Exceeding 115% and dropping below 40% requires a trip of after 100ms and 300ms, respectively; Reactive power regulation: Power factor ≤ 0,95.
Voltage stability: Large disturbance	Voltage limits during and after the fault for directly connected synchronous generators and other equipment are demonstrated in Appendix D.

It should be mentioned that the normal lower limit of voltage values is 90% of the nominal value. It can also be seen from voltage requirements during and after the fault, where the minimum voltage recovery level is precisely 90% (Ackermann, 2005). However, according to the chosen regulations, protection device settings do not include trip time for values less than 90%.

Thus, these stability conditions can provide the limits for installation at a particular grid point and be observed from the penetration index side. Based on them, stability analysis is carried out, and the limitations are mapped to indexes in a model.

3.4 Model

The model for testing stability is created in Simulink MATLAB software and represents a simplified 3-phase electrical network with three main blocks:

- Wind turbine, simplistically representing wind power plant, connected to a grid.
- Synchronous generator, performing the functions of conventional electricity producer in a grid and cross-border transfer flow from a neighborhood network.
- Load, which consists of several blocks and provides the system variable load and outgoing stream.

Also, these blocks contain 2-wing transformers with solidly grounded neutral, non-functional loads, which are necessary according to MATLAB demand and do not affect the model's processes and possibly short-circuit block. Additionally, the scheme contains additional elements, such as blocks for results computation. The overall system is shown in Figure 16.

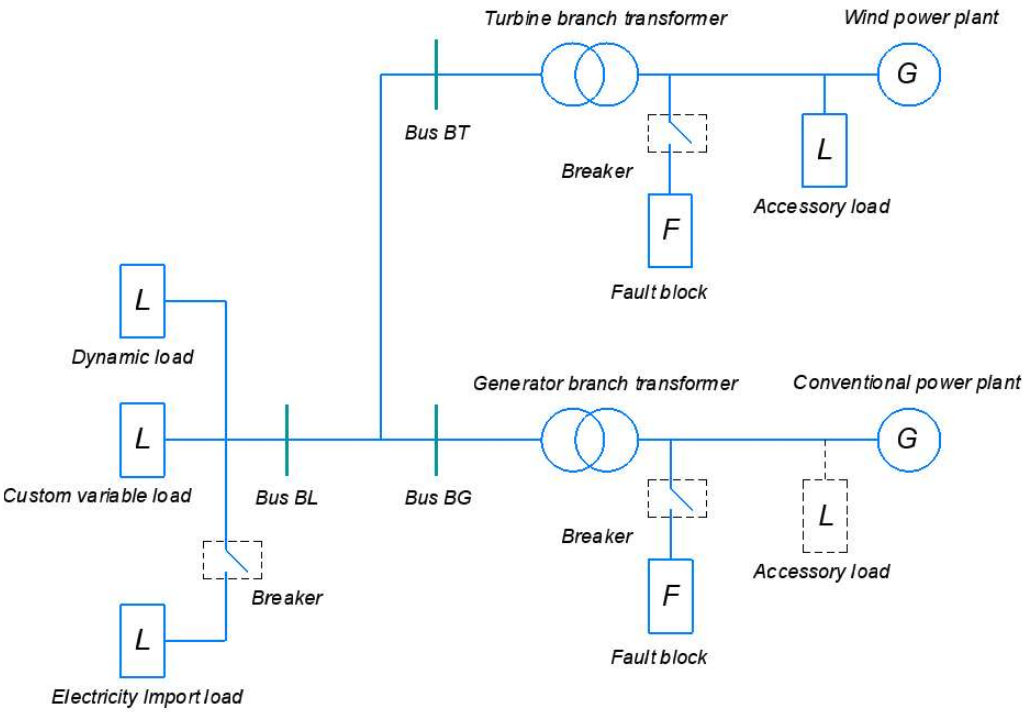

Figure 16 Model Diagram 1.

The following sections contain explanations of scheme blocks, where, for clarification, in addition to the methods for calculating the block values, examples and accepted provisions are also given. It is worth noting that the calculation is iterative. It also highlights which represented parameters are demonstrative and which are used in blocks.

3.5 Wind power plant branch

The main idea of the simulation is to test the effects of a rising share of wind power on grid stability. A Double-Fid Induction Generator (DGIF) wind turbine, represented as one block from the Simulink library, was chosen because it is the most popular type (Okedu, 2022). According to the source (The MathWorks Inc., 2023i), the block contains several inputs: 3 terminals for 3-phases current, trip, which is a logical input, and wind speed. The model's output is different conditions of the turbine, represented as a vector. The wind turbine model consists of 4 main sections: Generator, Turbine, Converter and Controller. So, the stator is directly connected to the network, and the rotor is connected to a grid through an AC/DC/AC converter and a coupling inductor. The parameters data are shown in Appendix E. The scheme of a wind turbine is shown in Figure 17.

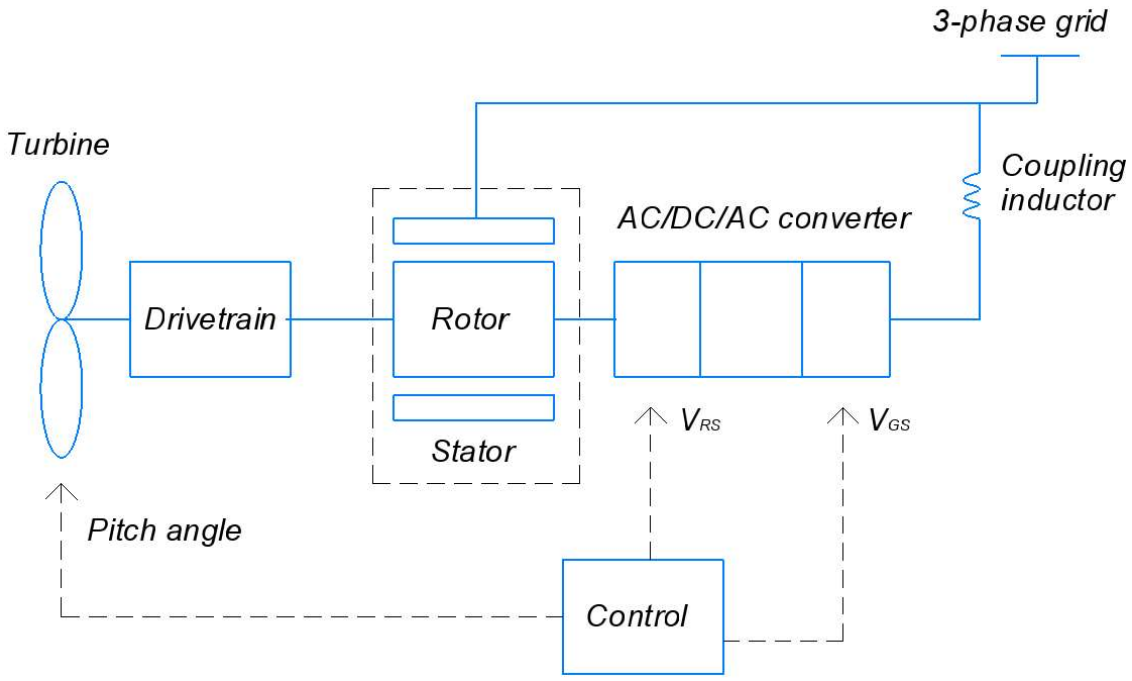

Figure 17 Schematic representation of a wind turbine. Adapted from (The MathWorks Inc., 2023i).

The turbine and generator tabs' parameters were taken from the source (Perelmuter, 2017) for 2MW nominal power wind turbine. The generator rating equals the nominal power divided by 0,95. This difference is necessary to get a turbine's maximum power (Simpson and Loth, 2022). Turbine power characteristics are shown in Figure 18.

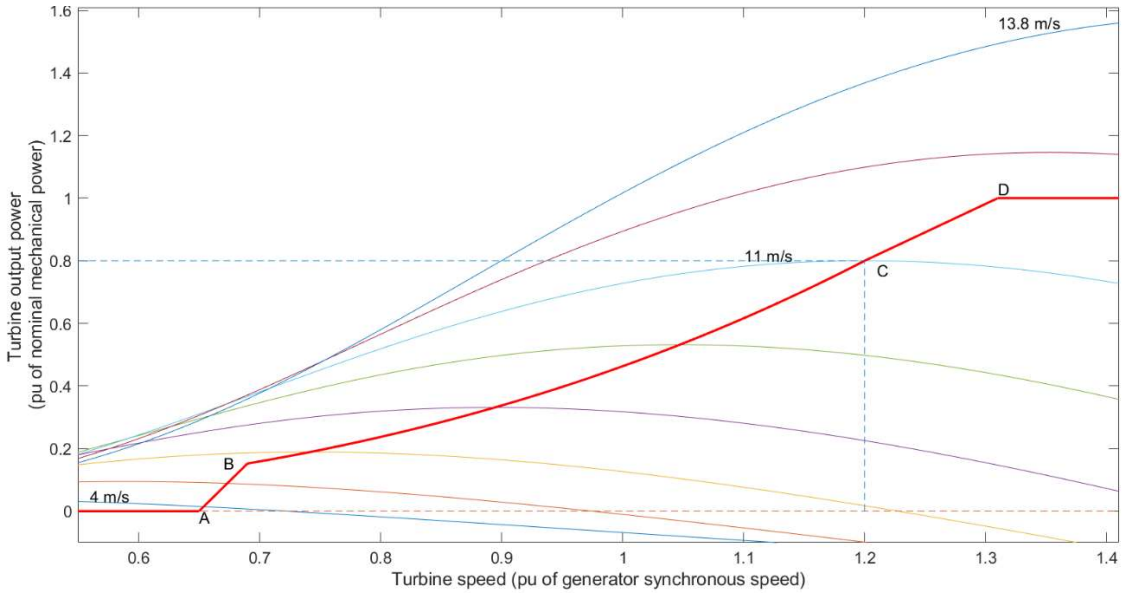

Figure 18 Wind turbine characteristic curve.

It should be emphasized that the wind turbine contains parameters in the "p.u." units, that is, a relative unit calculated as a parameter value divided by a chosen base value with the same unit.

The maximum converter power for the grid and rotor sides, contained in the converter tab, was chosen as a standard value of 0,3 p.u. of the nominal power (Perelmuter, 2017). The parameters of gride side inductor, in particular coupling inductance resistance and initial currents condition, and nominal bus voltage are assumed according to the source (Leila et al., 2017). Moreover, the last block's argument as DC bus capacitors is calculated according to Formula 10 from the source (The MathWorks Inc., 2023i).

$$\mathrm{C\ (F)} = \frac{S * 2 * t}{V_{dc}^2} \quad (10)$$

Where V_{dc} is nominal bus voltage, S is generator rating and t is a constant equal to 3-4 ms. (The MathWorks Inc., 2023i).

A detailed description of control systems is given in reference (The MathWorks Inc., 2023i). So, the wind turbine model includes pinch angle control, grid-side converter control and rotor-side converter control. All control schemes are represented in Appendix E. The rotor-side control provides power control, the tracking characteristic shown in Figure 18 by the red line, and voltage or reactive power control, which maintains the reference voltage value or amount of reactive power in a point of wind turbine connection. Grid-side control maintains the requirement voltage at the capacitor in the DC part of the

converter. Furthermore, pitch angle control regulates the attack angle of blades for adjusting a maximum power output (Earnest, 2019).

While setting the block, it is necessary to accept voltage or reactive power control. During the simulation, the first step is taking a voltage control regime with a reference voltage equal to 1 p.u. However, this regime does not limit the amount of produced reactive power, so if the power factor will not fit into the range from the grid code, the reactive power control regime with acceptance of the maximum possible produced reactive power is accepted. Evaluation of the acceptable value is going iteratively. The other values for the control tab are taken according to the source (Leila et al., 2017).

The wind turbine's nominal power is iteratively changed to evaluate the stability parameters with different penetration levels. So, as part of simplification, the generator rating, nominal power and DC bus capacitor are proportionally changed according to the required value analogous to the source (The MathWorks Inc., 2023h).

The wind speed is accepted as two ranges for 600 seconds each. The mean value of the first range equals 6,77 m/s, and the second is 12 m/s. These values are calculated separately according to the program, shown in Chapter 2.3. The first range allows checking the model during average wind conditions of the selected region (Global Wind Atlas 3.0, 2023). The second range tests for an upper production limit because, according to Figure 18, 12 m/s speed corresponds with the start of the maximum power output. The lower limit is not tested because:

- The MSWP indicates network problems at maximum wind energy load.
- The lower limit is restricted only by an ability to cover electricity shortage.
- One of the chapter's ideas is defining the penetration upper limit.

The mean value of 12 m/s is taken because it is a tiny more than the rated speed for the wind turbine. Also, it is evident that if the wind speed is higher, there will be fewer fluctuations and, therefore, less impact on disturbances. Looking ahead, the stability of large disturbances is tested at full load. At a lower wind speed, the number of periods when the turbine operates at full power is decreased, which also affects because the load of the entire system is variable. Thus, the value of 12 is chosen as an average compromise value. The wind speed is shown in Figure 19.

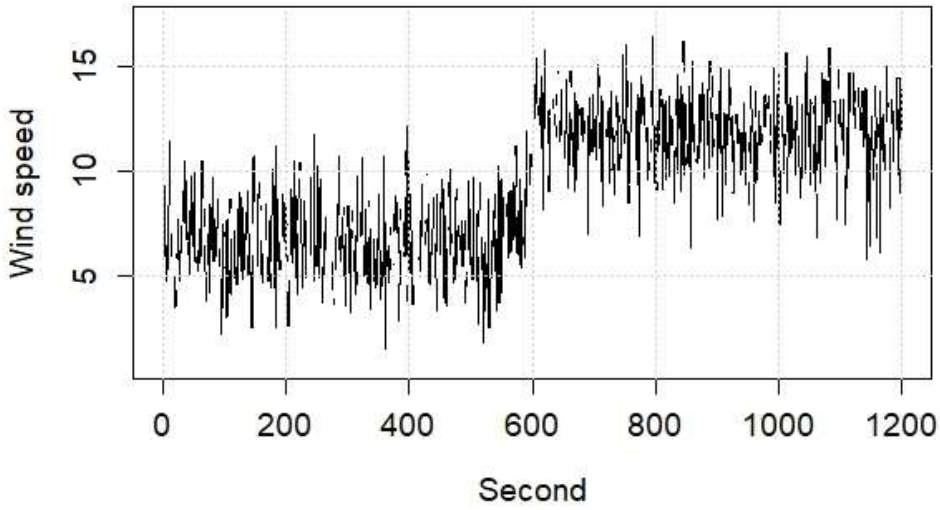

Figure 19 Wind speed test data.

Also, it is necessary to connect a small load, which has a negligible effect, in parallel with the wind turbine, only because of the Simulink logic. The load has an active power of 1kW. The block parameters are attached in Appendix E.

As was shown before, the current after the wind turbine typically faces two transformers, one at the turbine`s base for transmission of electricity inside a wind farm and another for connection of the wind plant to the grid (Earnest, 2019). However, to simplify, two transformers in the scheme have been replaced by one. So, was chosen a step-up 2-wing transformer with solidly grounded neutral. The connection type of the transformer is Y-Y, which is a cheap transformer type (Tikhomirov, 1986). Also, a solidly grounded neutral of low-voltage wing is chosen as the most widespread grounding type (Shipp and Angelini, 1988). Also, the low voltage is known according to the wind turbine, and the upper voltage is in the medium voltage level range, and it equals 33kV, due to chosen transformer model series, which is discussed further (Earnest, 2019). The next necessary point is nominal power for the transformer. The equation for nominal power calculation is shown in Equation 11.

$$P_{nT} = \frac{P_{nG}}{\eta} \qquad (11)$$

Where η is transformer efficiency, P_{nT} and P_{nG} are transformer and generator nominal powers respectively.

So, should be transformed the maximum power produced by the wind turbine. The nominal power value of a transformer is calculated as the turbine's generator power divided by transformer efficiency. According to the source (Tikhomirov, 1986)f, the transformer's efficiency is assumed to be 95% on average. Thus, when nominal power and both voltages are known, it is possible to accept a manufacturer or standard series

for a transformer. Based on the manufacturer 's data and after clarification of the power value, commonly applying the upper value and high voltage, extracted the following data (Perelmuter, 2017):

- The impedance of the transformer,
- No-load current,
- No-load losses,
- Short-circuit losses.

In this case, a series of transformers were chosen from the source (Tikhomirov, 1986). The received parameters are shown in Appendix E. Based on these parameters and according to the calculation method from the source (Perelmuter, 2017), the transformer parameters required by Simulink can be evaluated. The calculation method steps are represented in Equations 12 - 15.

$$Leakage\ inductance\ of\ 1st\ and\ 2nd\ widings, [pu]: L_1 = L_2 = \frac{0{,}5 * E_{sc}}{100} \quad (12)$$

$$Resistance\ of\ 1st\ and\ 2nd\ widings, [pu]: R_1 = R_2 = \frac{0{,}5 * P_{sc}}{P_{nT}} \quad (13)$$

$$Magnetization\ resistance, [pu]: R_m = \frac{P_{nT}}{P_{nl}} \quad (14)$$

$$Magnetization\ inductance, [pu]: L_m = \frac{R_m * (\frac{100}{I_{nl}})}{\sqrt{{R_m}^2 + (\frac{100}{I_{nl}})^2}} \quad (15)$$

Where E_{sc} is impedance voltage of the transformer in %, P_{sc} is short-circuit losses in W, P_{nl} is no-load losses in W and I_{nl} is no-load current in % (Perelmuter, 2017).

Calculated values and all blocks' parameters are represented in Appendix E. They are recalculated depending on the change in the rated power of the turbine during all tests, except for the efficiency of the selected transformer and series during the work. Hence, this work implements the calculation scheme with constant efficiency and chosen transformer series for all transformers calculated.

3.6 Synchronous generator

Synchronous generators are widespread in a network as a part of diesel generators, hydro turbines, and others because they produce reactive power and have a regulative

power factor (Christiaan Zuur, n.d.). So, the scheme contains a synchronous generator, but its nominal power combines synchronous generators and exchange capacities.

According to the source (The MathWorks Inc., 2023e) main block of the synchronous generator is represented by the Simulink block "Synchronous Machine pu Standard". This model is designed according to the standard (IEEE, 2020) and consists of an electrical and mechanical part, explained in Appendix F. The block contains inside prepared models of different synchronous generators, sorted by power and frequency. It allows using an example of a 50 Hz and 2 MVA rated power generator as a turnkey solution. The synchronous generator's nominal power value is changed by analogy with the wind turbine. Also, the block should be connected with 3-phase wires and has inputs of field voltage, mechanical power and output of multiple parameters describing the generator state (The MathWorks Inc., 2023e).

The field voltage input is taken as feedback based on "q" and "d" voltages values and transformed by the Excitation System block (The MathWorks Inc., 2023b). This block was created especially for the synchronous machine model as a modified "DC2A" exciter and included in the Simulink Simscape library block (IEEE, 1992). The main design differences of the exciter, compare to the standard, are:

- The Simulink system does not have exciter saturation,
- The Simulink exciter system has an input for additional oscillation stabilization,
- The terminal voltage transducer and load compensator work are based on "d" and "q" voltages compared to the Simulink model, where the device input includes current and voltage parameters.

Also, some parameters of transfer functions have changed compared to the standard. So, this block consists of the default values for the Simulink excitation system, produces direct current to the windings, and maintains a stable terminal voltage (The MathWorks Inc., 2023b). These two principal schemes are attached in Appendix F.

The mechanical power input is regulated by a governor block, which is not included in the Simulink library. This block is based on rotor speed reference value, expressed in p.u. units and produces mechanical power at the output. The block is a simplified governor block of a diesel generator, which can be implemented for the synchronous machine. This block taken from the source (Perelmuter, 2017). Its structure is shown in Figure 20.

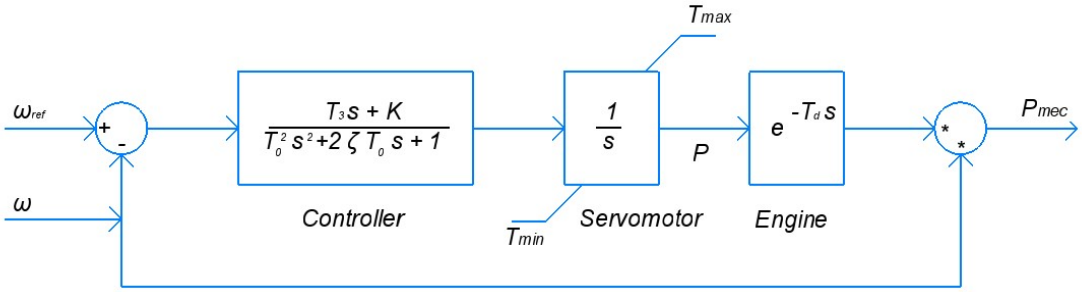

Figure 20 Governor block. Adapted from (Perelmuter, 2017).

The source (Perelmuter, 2017) describes the working principle of this block. So, the control block represents the second-order transfer function. Although an accurate diesel control model has a more significant transfer function order, this block approximates it well enough. An integrator block represents a servo motor, which allows for setting an initial value and saturation limits. A couple of these two blocks evaluate the torque of the generator. The last part of the system modulates a time delay for the whole block. Moreover, the system output is a multiplication between the torque and the speed, which equals mechanical power. So, the governor maintains a stable value of the rotor speed and, changing the torque, allows the production of the demanded power. The whole block´s values are demonstrated in Appendix F.

At the exit of the branch, the synchronous machine is connected to a transformer. The transformer parameters' evaluation method and initial positions are calculated similarly to what was discussed above with the same chosen manufacturing series.

3.7 Loads and additional equipment

The load branch consists of 3 main parts: Dynamic load, Transfer capacity and Variable load. The dynamic load is a Three-Phase Dynamic Load block placed in the Simscape library of Simulink library and described in the source (The MathWorks Inc., 2023f). The main idea of this block is that active and reactive load power can vary according to equations 15 and 16, respectively, in case the voltage exceeds a set limit. Also, the impedance is constant if the voltage is lower than the range voltage. Equations 15 and 16, according to the source (The MathWorks Inc., 2023f), are represented below.

$$P = P_0 \left(\frac{V}{V_o}\right) \quad (15)$$

$$P = P_0 \left(\frac{V}{V_o}\right)^2 \quad (16)$$

Where P is an active power, V_o is an initial voltage, and P_0 is an initial voltage (The MathWorks Inc., 2023f). Equation 15 describes a situation when voltage exceeds the set limit. In this case, the current is constant. Equation 16 is for problems when voltage is below the limit voltage value. In this case, impedance is kept constant. For reactive power, the equations are the same. This block is necessary for the scheme because it helps to connect variable electricity production and consumption more smoothly. The Dynamic block requires entering initial active and reactive powers, a frequency, an initial voltage, the limit voltage, and equations parameters (The MathWorks Inc., 2023f). The block is shown in Appendix G.

Transfer capacity, which absorbs electricity for balancing purposes, represents by a series RLC load block with a three-phase breaker, which connects it at a suitable time. The load block is connected at 601st second when the generation from the wind turbine will be excessive due to increased wind speed. The RLC load constantly consumes active power from this time, which equals the calculated transfer capacity.

The final part of the load blocks is a block with a time variable load. The block was designed according to the source (The MathWorks Inc., 2023a). It is not included in the standard Simulink library. The load consists of the electrical scheme and the evaluation part. The electrical part creates a current in a 3-phase balanced system based on two current sources: A and B phase components, two voltage measurement blocks, which measure lines voltage for the feedback in a calculation scheme, and two resistors. The scheme is shown in Figure 21.

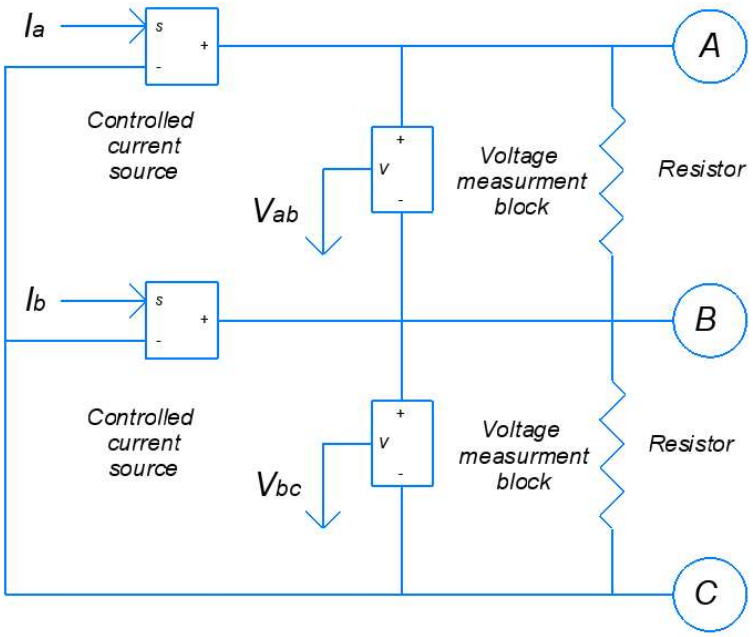

Figure 21 Electrical part of variable load. Adopted from (The MathWorks Inc., 2023a).

The inputs are A and B phase peak currents, and the output is AB and BC peak line-line voltages, all in complex form. The peak values are necessary for the source blocks, which require initial states, such as the current's phase, amplitude, and frequency. The resistors' resistance is set equal to 1 million Ohms for phase separation. According to the initial assumption that the system is balanced, and vectors are in positive sequence form, these parameters are sufficient to create a 3-phase current. The calculation scheme is based on the following equation (The MathWorks Inc., 2023a):

$$S = \frac{3 * (V * I')}{2} \quad (17)$$

This is a standard equation of the Complex power with peak current and voltage values, where I´ is a conjugate of a complex current (Chapman, 2011). So, this formula links input current and output voltage. Figure 22 demonstrates the block diagram of the whole calculation circuit.

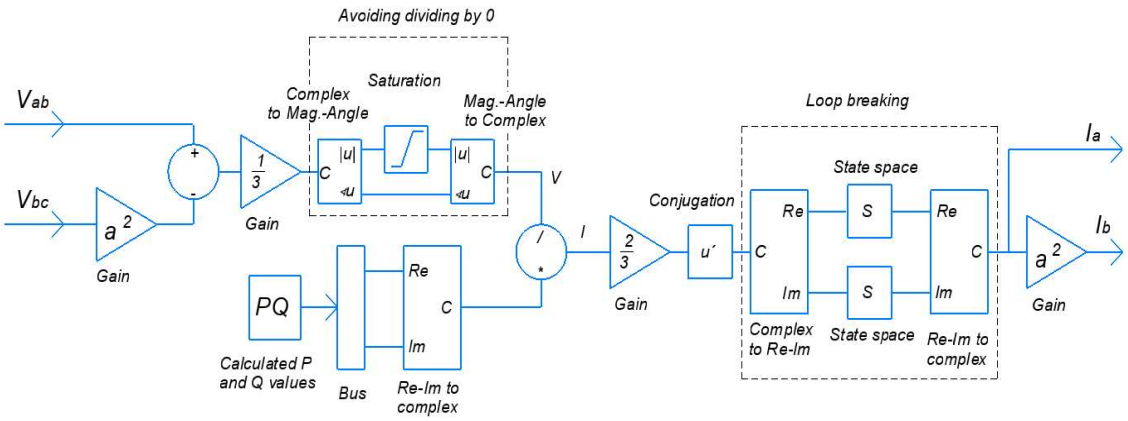

Figure 22 Calculation scheme of variable load. Adopted from (The MathWorks Inc., 2023a).

So, the main idea of the circuit is that the Complex power, divided by the voltage and coefficient according to formula 17, is equal to the current. However, it is necessary to add some transformation for getting a phase current from the line voltages. Initially, line-line voltages should be recalculated according to equation 18. Equations 17 and 18 are represented below (The MathWorks Inc., 2023a).

$$V_a = \frac{(V_{ab} - a^2 * V_{bc})}{3} \quad (18)$$

$$a^2 = e^{-j*\frac{2*\pi}{3}} \quad (19)$$

Where V_a – is A phase voltage, V_{ab} and V_{bc} are line-line voltages, a^2 is phase shift to minus120 degrees. The derivation of this equation is attached in Appendix G.

So, a phase voltage is obtained. After that, the A phase current is calculated as follows: The complex power, which is discussed below, is divided by the voltage and the ratio, and for the resulting value, the conjugate is also performed. Also, before injecting the current values into a system, it is necessary to solve an issue of an algebraic loop, which is done by implementing two state-space blocks with a damping effect for both imaginary and real parts of complex input signals (The MathWorks Inc., 2023a). These block values are shown in Appendix G. Finally, the B phase current is calculated as the A phase current with a shift of -120 degrees.

The complex power is set according to active and reactive power and united in 1 complex value at the end. The diagram of the setting assuming active and reactive power is shown in Figure 23.

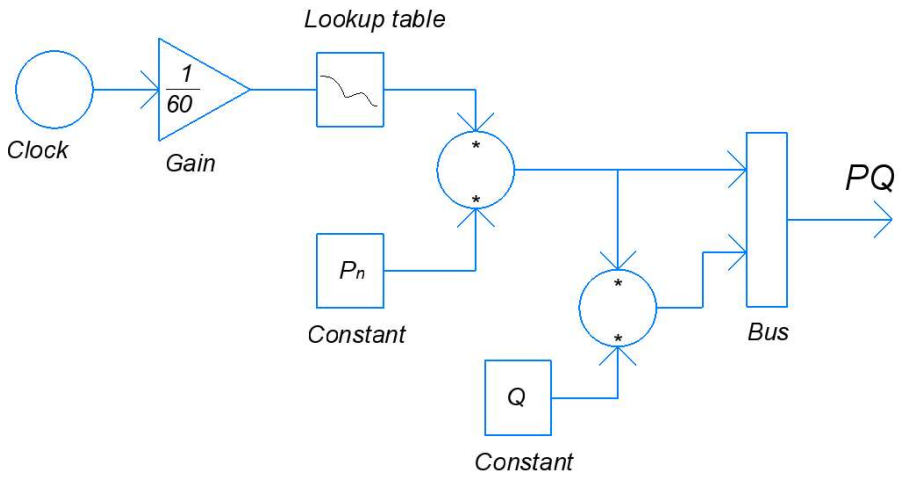

Figure 23 Power evaluation scheme of variable load. Adopted from (The MathWorks Inc., 2023a).

Nominal active and reactive powers are configuring parameters. The reactive power consumption by the load is set to 0 for simplicity. The reactive power inside the scheme can be used for active power transmission and, sometimes, for wind turbine consumption. The lookup table block contains a 1-minute consumption profile downloaded to Simulink from outer, which are transferred to 1-second values by linear extrapolation. For evaluation of possible consumption, the shape was chosen the dataset with a 1-minute resolution according to the source (Open Power System Data, 2020), which provides household data from business, public and residual buildings in Konstanz. According to the simulation duration and purpose, a typical working day was chosen to investigate possible electricity fluctuation during a day and evaluate a base load level. A

dimensionless consumption curve was obtained based on it. The curve is shown in Figure 24.

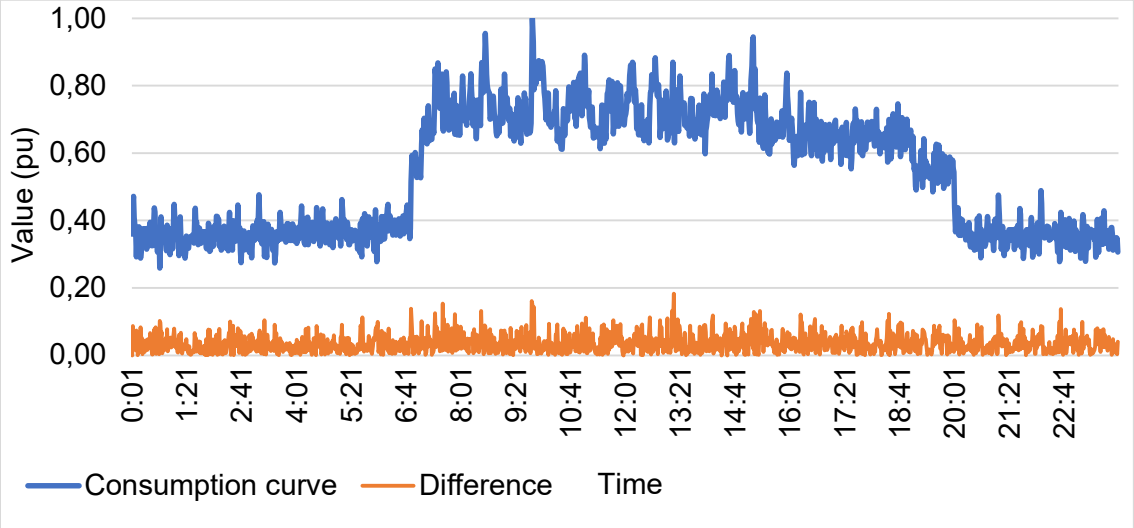

Figure 24 Day load profile.

According to the data, the base load is evaluated as 0,27 p.u., used in the Dynamic load block. Also, the maximum change in 1 minute is 0,18 p.u., and the maximum value is one p.u. For correlation with the wind speed data, the consumption profile is adjusted and divided into two parts for average and high-speed data, but in reverse order with respect to wind speed for testing the limit cases. So, the central part of the load curve, where the consumption is maximum, is used for the initial 600 seconds, and the initial part of the curve is used for the other 600 seconds. Additionally, both ranges include top changes. The resulting consumption profile consists of 20 values for 1 minute, which are two ranges of real data, 9:43 to 9:52 and 3:28 to 3:36. The 10th and 11th values are manually calculated for connections between the ranges and represent the maximum changing periods. These values are used in the lookup table block. The result consumption data is shown in Figure 25.

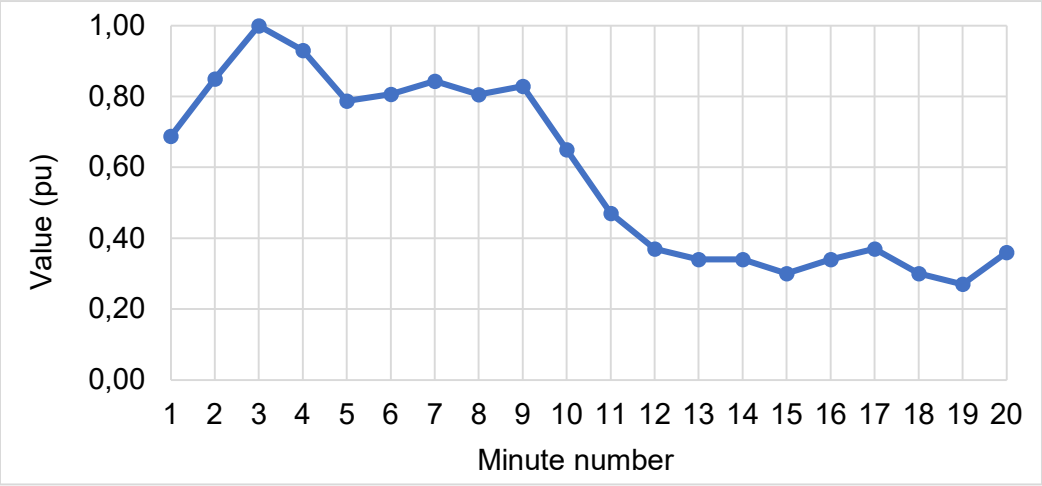

Figure 25 Consumption curve.

The additional necessary equipment consists of short-circuit blocks and a „Powergui" block. Short-circuit blocks are added for tests. They have connected nearby the synchronous generator for large disturbance voltage and transient stabilities checking and around the wind turbine for large disturbance voltage stability investigation. According to the regulations, the short circuit duration equals 150 ms. The short circuit should be made when the equipment is under the maximum load (Meegahapola and Flynn, 2010). Also, the scheme contains the essential "Powergui" block, which provides calculation processes. The calculation regime was chosen „Phasor" because it is demanded by wind turbine block. Finally, when all equipment is described, it is possible to start a simulation and obtain results.

3.8 Simulation and results

The simulation investigates the wind capacity, which can be connected to a system respecting the grid stability criteria. Thus, according to the sources (Shi et al., 2011), the plan is initially to create stable systems with only conventional power according to the stability criteria and inject wind power with implemented variable wind speed into the network.

The following data are necessary for the start of the simulation:

- Wind speed data,
- Load capacity,
- Transfer capacity,
- Turbine nominal power,
- Synchronous generator power.

The fluctuated wind speed data is generated before and shown in Figure 19. The maximum load capacity is 10 MW, where 2,7 MW is a base load inside the Dynamic Load block and the rest is the variable load. The consumption curve, shown in Figure 25, remains the same according to the previous subchapter. The value of 10 MW was chosen because when working with a smaller load, problems arise with the program calculation of the short circuit. The export capacity is entered into the model when the nominal power of the wind turbine exceeds the base load and equals to their difference, which is the MSWP index of 100%. Before this moment, the exchange capacity equals 0. The values of the turbine and the generator power are the key figures which define the indexes, and they are assumed by the iterative method. All steps of iterative methods are made by taking into attention the regulations, which are mentioned in Chapter 3.3.

The following disturbance signals are used in this model, when possible:

- The load profile in the form of ramp signals and the step wind change, which cause turbines power output change, are used as the small disturbances according to the sources (Toma et al., 2021) and (Chouket and Krichen, 2015), respectively. Additionally, the variable wind speed is implemented in the model.
- The Large disturbance is implemented by the short circuit block, which is placed between the generator and the following transformer. The short circuit duration is 150 ms. (BDEW, 2008).

The first step is defining a stabilized system with 0 levels of wind energy penetration. For this reason, the load is set as the maximum value of 10 MW, the turbine branch is disconnected from the scheme and the synchronous generator is investigated. The 10 MVA synchronous generator model is initially applied, and the rated power is increased until consumption is satisfied. The load curve is attached in Appendix H. The whole test lasts 60 seconds, where the growth ends at 20th seconds, and the short circuit fault happens at 40th seconds. These intervals are sufficient for the system to stabilize after disturbances. The short circuit block implements a symmetrical fault, mainly a 3-phase short circuit fault to ground. The location of the fault is the closest to the tested equipment, which is fully loaded. According to the sources (Meegahapola and Flynn, 2010) and (Kumari et al., 2016), all these conditions realize the worst case. The same short circuit type is applied to the wind turbine. The observation goes by the buses "BL", "BG", and "BC" for the identification of the worst cases. The bus "BL" also obeys the same regulation, although it is the load bus. Because, German technical-scientific associations VDE provide the same grid code for demand and supply connections, which is taken as a simplification in this work (VDE, 2018).

The 10 MVA is enough to be within limits during the small disturbance cases. However, the 10.18 MVA capacity precisely compensates for all losses and produces enough reactive power to operate on exactly 50 Hz. Nevertheless, during the short circuit, these power values do not meet the short-circuit requirements of time and voltage for a directly connected synchronous generator, attached in Appendix D. Thus, the first accepted value, which meets all requirements, is 11,5 MVA. Also, it should be noted that the generator is loaded up to 99.8% of its capacity during the test. The result of the fault test is shown in Figure 26.

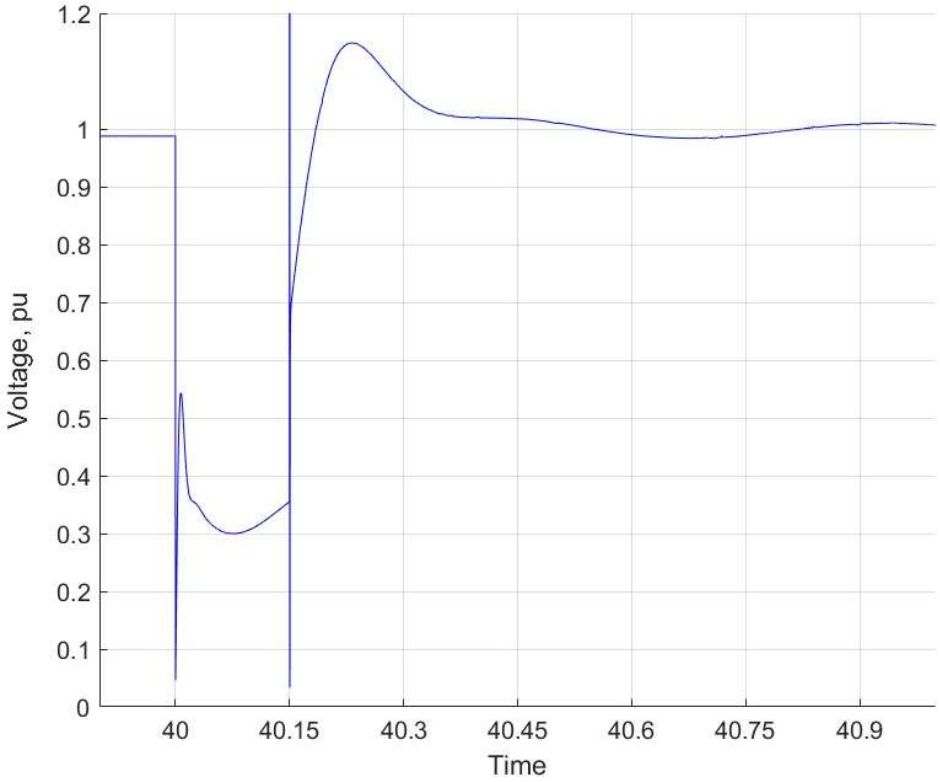

Figure 26 Initial evaluation, large disturbance test.

Also, it should be emphasized that the maximum power factor of the generator is 1, which means that the generator's capacity can be equal to its nominal power. So, in terms of the generator, it is possible to convert MVA to MW for the generator directly.

The following steps are the investigation of wind penetration level, which can be implemented in 2 ways (Meegahapola and Flynn, 2010):

1. Increasing the wind turbine's power while maintaining the generator's power unchanged. So, the total capacity is increased, and the load on the generator is reduced.
2. Rising of the wind turbine capacities with simultaneous reduction of generator power. The overall capacity is constant.

Initially was observed the method with total capacity increasing. The first step is calculating the turbine power limit regarding stability criteria. As a result, the 5,3 MW power for the turbine is the maximum possible value in terms of stability for small signal cases. For the rest of the tested parameters, this power is not critical. The maximum reached frequency is 51,52 Hz, but the excess duration is less than 100 ms., so it does not lead to disconnection (BDEW, 2008). Further increasing of turbine nominal power will shut down the wind turbine. The frequency values fluctuation is shown in Figure 27.

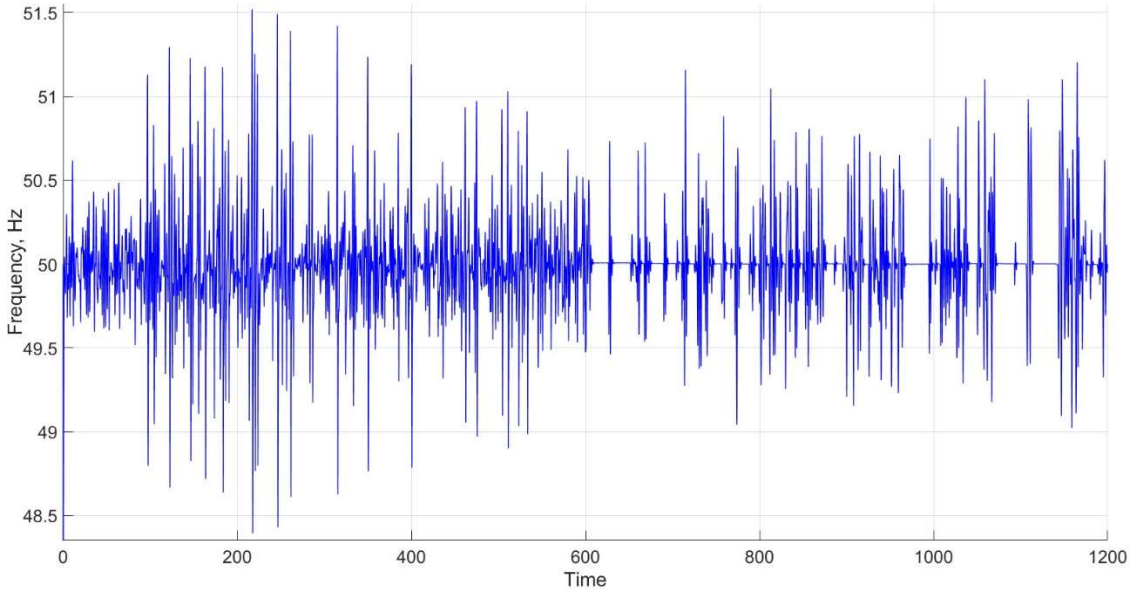

Figure 27 Frequency fluctuations in the limiting case.

Also, according to the stability requirements and due to the absence of severe losses in the scheme, the nearest critical limits for frequency and voltage fluctuations with small disturbances are the upper limits. So, they are shown in resulting tables. The maximum reached voltage value is 1,054 p.u. This graph is attached in Appendix H. The load angle was not close to the critical value, and its most significant value equals 64 degrees. The load angle values are demonstrated in the graph, which is also attached in Appendix H.

The tests with large disturbances were made with maximum load by analogy with the preliminary test explained above but with two variants of 3-phase faults: in turbine and generator lines. The maximum consumption is increased to 15 MW to meet the complete loading condition because the turbine can produce up to 5,3 MW due to the PF.

As a result, after the transient stability test, the maximum load angle was 177,54 degrees, and the minimum TRASI index was equal to 0,598 at the short circuit on the line of the synchronous generator. These values also are not critical.

The time-voltage restrictions are also respected. But, the short-circuit in the turbine lines had the most negative impact than the fault in the generator line for large voltage disturbance tests. So, the maximum output duration to a value of 0.9 of the rated voltage is 0,7 seconds after the short-circuit fault starts, but the curve lies between two border lines in the case of the turbine line, which is not a good result. For the fault on the generator line case, the time characteristics are good, and the break-off point lies at 0.8+ p.u., demonstrating a margin. The load angle curve and time-voltage graphs are attached in Appendix H. For comparison, corresponding test values of several wind power penetration levels are shown in Table 5.

Table 5 Addition method.

Wind turbine nominal power, MW	2	3	4	5,3
Small signal cases				
Max. voltage, p.u.	1,01	1,01	1,03	1,05
Max. Frequency, Hz	50,45	50,63	50,89	51,49
Max. load angle, degrees	53	55	57	57
Large signal cases				
TRASI	0,577	0,573	0,563	0,554
Max. load angle, degrees	178,3	177,7	178,7	177,8
Initial voltage (worst case), p.u.	0,85	0,83	0,84	0,8
Time (worst case), seconds	0,78	0,78	0,77	0,70
Indexes				
WEP, %	19,03	28,89	38,84	51,76
WCP, %	20	30	40	53
MSWP, %	74	100	100	100

The Initial voltage is a voltage recovery value after the fault, and time is the voltage input time in the 0.9 p.u. range. The Transfer capacities for MSWP value are calculated according to the previously described logic.

The next step is the implementation of the replacement method. So, the total nominal power remains constant, and an increase in the turbine capacity equals a decrease in the generator capacity. The maximum consumption equals 10MW for all tests. The results are demonstrated in Table 6.

Table 6 Substitution method.

Wind turbine nominal power, MW	0,5	1	1,5
Synchronous generator nominal power, MW	11,0	10,5	10,0
Small signal cases			
Max. voltage, p.u.	1,01	1,02	1,02
Max. Frequency, Hz	50,12	50,25	50,38
Max. load angle, degrees	52	54	56
Large signal cases			
TRASI	0,583	0,586	0,585
Max. load angle, degrees	179,8	178,4	179,2
Initial voltage (worst case), p.u.	0,59	0,52	0,30
Time (worst case), seconds	0,18	0,19	0,52
Indexes			
WEP, %	4,42	4,64	4,71
WCP, %	5	10	15
MSWP, %	18,5	37,0	55,6

A feature of this method is that the generator works in all 3 cases at a load close to 100%, in the first 600 seconds and during the tests with the fault. Also, the maximum frequency and voltage fluctuation values were reached in the second time interval, particularly from 600 to 1200 seconds. However, applying the substitution method is impossible based on the requirements due to the voltage's low received recovery values. As was shown in the defining of the initial generator value and additionally tested in this case, the value of voltage recovery after the fault reaches 0,7+ p.u. only when the synchronous generator rating equals 11,5+ MVA.

So, according to the table data, increasing the wind penetration level affects the system stability negatively under small disturbances, which agrees with the conclusion given in the sources (Meegahapola and Flynn, 2010) and (Edrisian et al., 2014). The ranges of the voltage and frequency fluctuations and the maximum load angle of the synchronous generator are increased during the growth of the wind energy penetration level. All of them are consequences of output power fluctuations from the wind turbine and the generator's response to stabilize the system.

A slightly different tendency is demonstrated in large disturbance voltage stability tests. The voltage starting values rise with decreasing in the turbine capacity. The situation is reversed with the time values, where increasing the wind power improves the time characteristics. Although, these values are much less than the critical value compared to the voltage values that define the limit. Finally, based on the 2 cases studied and the source (Meegahapola and Littler, 2015), it was demonstrated that wind power penetration is not the only determining factor for this problem, although it is important.

Nevertheless, the transient stability tests show other results. Although the demonstrated cases satisfy the reliability requirements, the TRASI index signalizes a minor increase in system reliability with the growth of wind penetration. But, according to the source (Meegahapola and Flynn, 2010), wind penetration intensify the system's behaviour during transient stability rather than determining its direction. Moreover, it seems an objective conclusion considering two investigated cases and a minority of changes.

So, the WEP and WCP indexes calculated for each case can be used as the criteria of limitation of the possible wind penetration level in terms of stability, but with necessary additions. As was shown before, these indexes can define the limits under criteria of frequency and small disturbance rotor angle and voltage stabilities, but not to the large disturbance stability, which only depends a little on the indexes. Finally, if the transient stability issue is delegated to other criteria, in that case, operating the WEP and WCP indexes as limiting factors in terms of stability with an assumed error level is possible. Also, careful network modelling is needed. The MSWP index, based on the reasonable assumption of avoiding the loss of generated electricity, definitely makes it easier to model networks and allows one to limit the possible installed variable renewable capacity but not in terms of the stability analysis.

4. SCR

The chapter discusses the "Grid strength" and SCR index. In particular, research was done on the relationship between the index and network stability by analysing stability and creating a Simulink model. The influence of the reactance-to-resistance ratio on the grid is also considered. As a result, the influence on the network stability and possibility of wind-installed power in valuation in a connection point were demonstrated based on the data obtained.

4.1 Grid strength

The grid strength is the characterization of the network in a point and represents the overall power of the short circuit (Golieva, 2015). This parameter is described based on the network and the equipment's capacity. So, the grid strength definition means interaction between the grid and the source or load connected to the network (Xu et al., 2023).

The numerical determination of this parameter requires several steps. Initially, for the connection of a wind power plant and situation assessments, using Thevenin's theorem, it is necessary to calculate the Short-Circuit Power at a PCC (Golieva, 2015). The SCP equals the ratio between the squared voltage at the PCC point and the equivalent impedance (Clausen, 2013). This is shown in Formula 20.

$$\mathrm{SCP} = \frac{\mathrm{V}}{\mathrm{Z}} \quad (20)$$

Where V – is a voltage in PCC and Z – is equivalent impedance. The SCP is measured in VA (Clausen, 2013).

The final stage includes a Short-Circuit Ration index calculation based on the plant's SCP value and nominal production power. This index allows one to conclude the grid strength. The SCR equals the ratio between a grid Short-Circuit Power in the numerator and the nominal power of grid-connected equipment in the denominator. This equation is shown in Formula 21.

$$\mathrm{SCR} = \frac{\mathrm{SCP}}{\mathrm{P_n}} \quad (21)$$

Where $\mathrm{P_n}$ – is nominal power. Additionally, as mentioned earlier, the voltage at the PCC is selected for reasons unrelated to this index.

Thus, by defining the SCR ratio, it is possible to determine the weakness or strength of the grid. According to the source (Earnest, 2019), there are three main ranges :

- SCR ≥ 20. This value of SCR indicates that it is the “Strong” grid case, and the power system can be easily connected to the network.
- 10 ≤ SCR ≤ 20. If the index fits into this range, the connected wind plant should participate in grid control.
- SCR ≤ 10. This is a sign of the „Weak” network, and the chosen capacity of the wind plant is not recommended for installation.

So, the SCR index is a „grid side“ parameter which defines recommendations for the planned grid-connected electricity producer, which can also be interpreted as an upper limit for the power connected to the network.

Another important parameter is the ratio between reactance and resistance, called the impedance phase angle. This parameter affects the deviation of the voltage value at the connection point (Tande, 2000). Also, the minimum allowable value of SCR in any particular case varies on a network's X/R ratio (Reginatto and Rocha, 2009). So, according to these articles, the SCR value is considered together with the X/R ratio. Hence, the ratio is observed in this chapter.

A Simulink model of a grid-connected wind turbine was created to investigate the relationship between the indexes and the stability of the network and the possibility of determining the maximum value of grid-connected power in a particular case. The model explored changing of the frequency and voltage parameters.

4.2 Model

The model represents a 3-phase grid-connected wind power plant. This model is a modification of the previous scheme shown in Chapter 3. So, the turbine line, which includes the wind turbine, additional load and the transformer, remains the same, but the turbine's nominal power of 2 MW as in its original form. The remaining scheme part, in particular the generator and the consumer parts, were replaced by the source block, which implements the grid as a whole unit. The model is demonstrated in Figure 28.

The source block, explained in the reference (The MathWorks Inc., 2023g), is a 3-phase voltage source with internal impedance. This block allows setting the short circuit power and X/R ratio in a point after the source, which is a PCC point according to the scheme (The MathWorks Inc., 2023g). Also, according to the previous system, this block contains voltage and frequency parameters, particularly 50 Hz and 33kV. Also, an initial phase angle is set to 0 for simplification. The source parameters are attached in Appendix I.

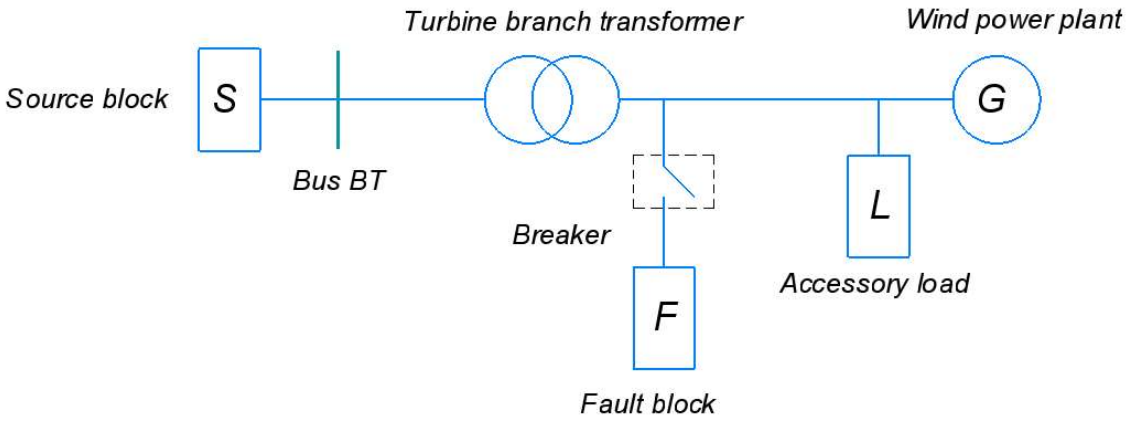

Figure 28 Model Diagram 2.

4.3 Simulation and results

The research is divided into two main parts:

- Research of general influence from SCR and X/R indexes. In this subchapter, the wind speed is constant and equals 12. Research is being carried out by changing the SCP and X/R parameters of the source block with a constant power of the wind turbine.
- Finding the maximum possible connected wind power according to the stability requirements. The SCP and X/R values of the source are fixed. The regulation limits are the same as in Chapter 3, but with a focus on the voltage ranges for large and small disturbances and the frequency fluctuation limits. The large disturbance source is taken according to the previous chapter, which is the 3-phase short circuit. The abrupt change in the turbine power output due to the change of mean wind speed, and the general variable wind speed nature with maximum turbulence, are considered small disturbances (Chouket and Krichen, 2015).

4.4 General influence

For the first part, as mentioned before, 2 MW of the nominal turbine power is assumed, the SCP equals 40 MVA as the minimum SCR value of a strong grid, and the X/R ratio equals 10 as a default. So, the X/R value is fixed, and the SCR value decreases gradually until parameters are out of the allowable range. The observed SCP and corresponding SCR ratios are demonstrated in Table 7.

Table 7 SCR testing levels.

SCP, MVA	40	20	10
SCR	20	10	5

Represented value demonstrates the transition from a strong grid to a weak grid. The comparison of the influence is shown in the following parameters, according to the source (Golieva, 2015):

- Voltage value at PCC, which demonstrates the transfer capability of the active power.
- Reactive power production from the wind turbine. It also affects the voltage level at PCC.

Additionally, two regimes of wind turbine controls, such as voltage and reactive power controls, are considered. These two regimes are described in Chapter 3. The voltage changes at PCC are shown in Figure 29. The graph starts at 10 seconds to discard some of the fluctuation caused by initialization.

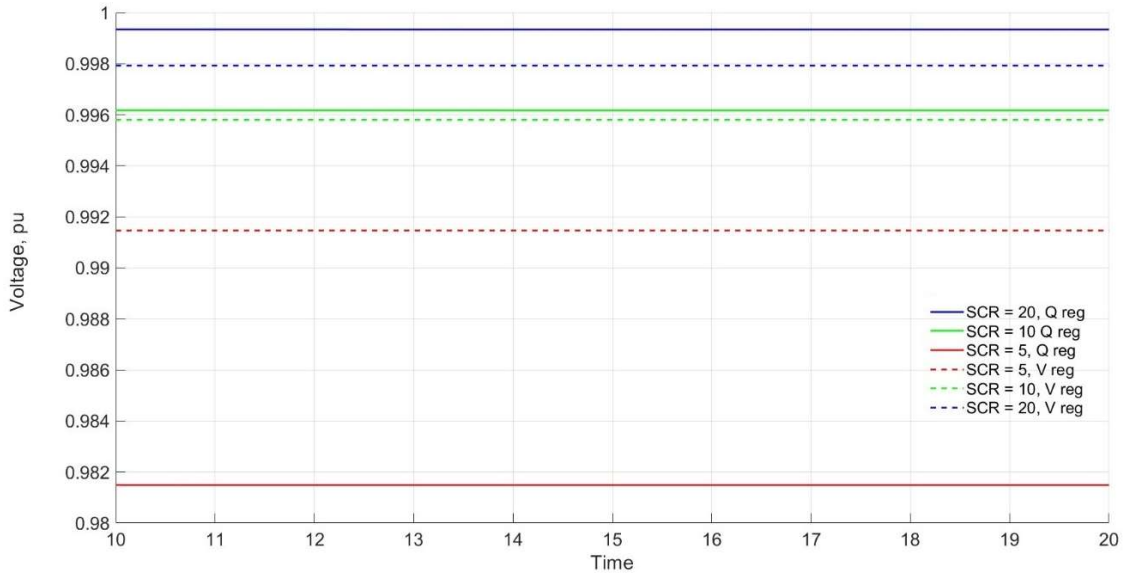

Figure 29 Variable SCR, voltage values.

It is seen that the reduction of SCR decreases the voltage level at PCC and, as a result, the transmitted active power is decline (Golieva, 2015). Also, there are distinctions caused by the regulation types. Nevertheless, the voltage value generally differs from 1 p.u. in the case of the strong grid due to the inner losses, calculation errors and, if applicable, voltage regulation, which is focused on the point after the wind turbine.

The next test cases observe the supply of reactive power by the wind turbine, which also affects the voltage level at PCC. Everything is evident for the case with chosen reactive power regulation - the reactive power production is zero. An increase in reactive power production is observed for the voltage regulation regime. So, when the grid is strong, the reactive power consumption allows maintaining the voltage at a level close to 1 p.u. However, reducing the SCR value requires reducing reactive power usage for wind turbines. Furthermore, the turbine must produce reactive power with a further decrease in the index. These observations are represented in Figure 30.

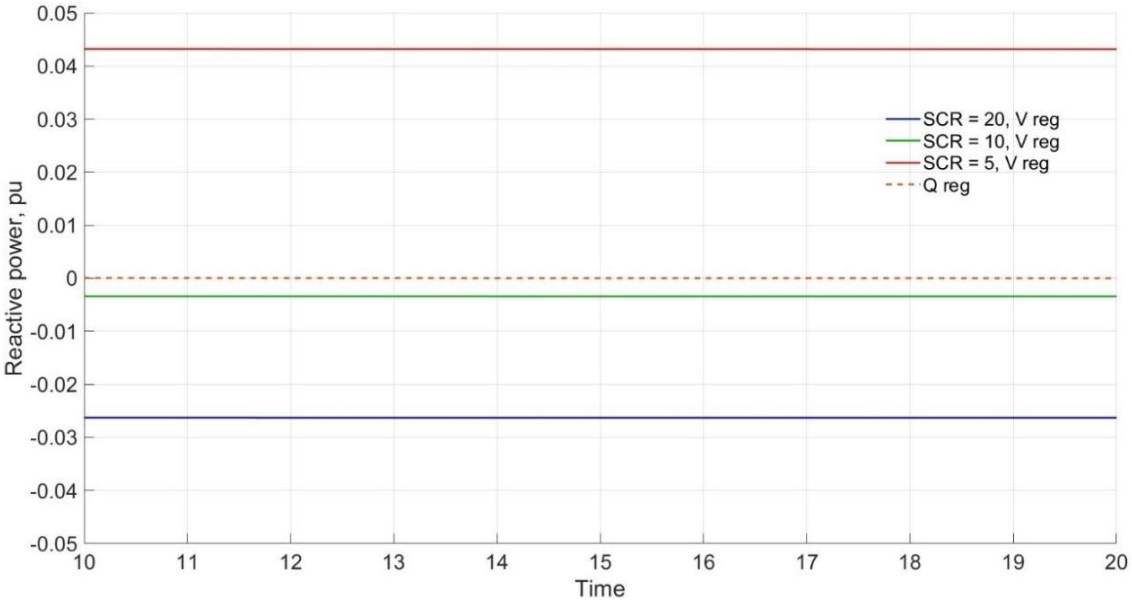

Figure 30 Variable SCR, reactive power production.

Also, it was found that the minimum SCR value depends on the regulatory regime. On the one hand, the voltage regulation regime has a 2,25 minimum value for the SCR because further decreasing causes considerable fluctuations in the system during the attempt to maintain voltage. On the other hand, the reactive power regulation has a minimum value of SCR equal to 2 because the continuation of the SCR value decline leads to a prolonged drop voltage at PCC below 0.8 p.u., which is not allowed by the regulator. Thus, considering both observations, it can be concluded that decreasing SCR value negatively affects the maximum transferred active capacity.

In the same way, the influence of the X/R ratio is tested. Each SCR level, tested before, was calculated voltage levels at PCC with different X/R ratios. Also, were tested both control regimes of the wind turbine. The calculated values are shown in Table 8.

Table 8 X/R calculated values.

	SCR = 20		SCR = 10		SCR = 5	
X/R ratio	V control	Q control	V control	Q control	V control	Q control
1	1,021	1,042	1,026	1,080	1,026	1,142
5	1,001	1,005	1,001	1,007	0,999	1,005
10	0,999	1,000	0,997	0,998	0,995	0,985
20	0,997	0,998	0,996	0,993	0,992	0,975
50	0,996	0,996	0,995	0,990	0,991	0,968

So, according to the results, it is clearly seen that increasing the X/R ratio worsens the voltage value and hence decreases the maximum transferable active power. Also, the X/R ratio enhances the trend, in particular, X/R values have a more significant influence on a weak grid than a strong one (Golieva, 2015). For example, the voltage of the weak grid is more powerful than the voltage of the strong grid, where the X/R ratio equals 1 for both of them. All of it is relevant for both control regimes. So, that means that the X/R ratio should be considered with the SCR ratio for the grid parameters investigation.

4.5 Searching for the limit

In this case, the stability analyses are conducted to test the SCR factor with a known X/R ratio as a limiting factor for installing maximum grid-connected power in a specific region. The grid, represented by the source block, has the SCP equals to 1000 MVA, which approximately correlates with the connection's voltage level (Navarro, 2021a). The X/R index equals 10 as the common value for this voltage level (Vilmann et al., 2023). The increase in wind turbine capacity occurs in the same way as in the previous chapter. Also, the zero-production wind turbine reactive power control mode is chosen to meet the power factor requirements.

The small disturbance test shows that the maximum possible turbine power is 465 MW. So, the reason for the limitation, in this case, was the voltage value at PCC. During the time interval of the maximum turbine production and, consequently, at a lower SCR value, the voltage dropped below 0.8 p.u., but its duration was less than 2,7 s, so the wind turbine has not disconnected. However, further increasing of wind turbine power

will lead to turbine disconnection. As a result, the conclusion of the first part was confirmed. Also, the difference in stability between a weak and strong network was demonstrated. So, power fluctuations create more significant voltage fluctuations in the grid with lower SCR than in the network with a higher SCR value. All of it emphasizes the importance of the SCR parameter. The voltage behaviour at PCC during the wind fluctuations is shown in Figure 31.

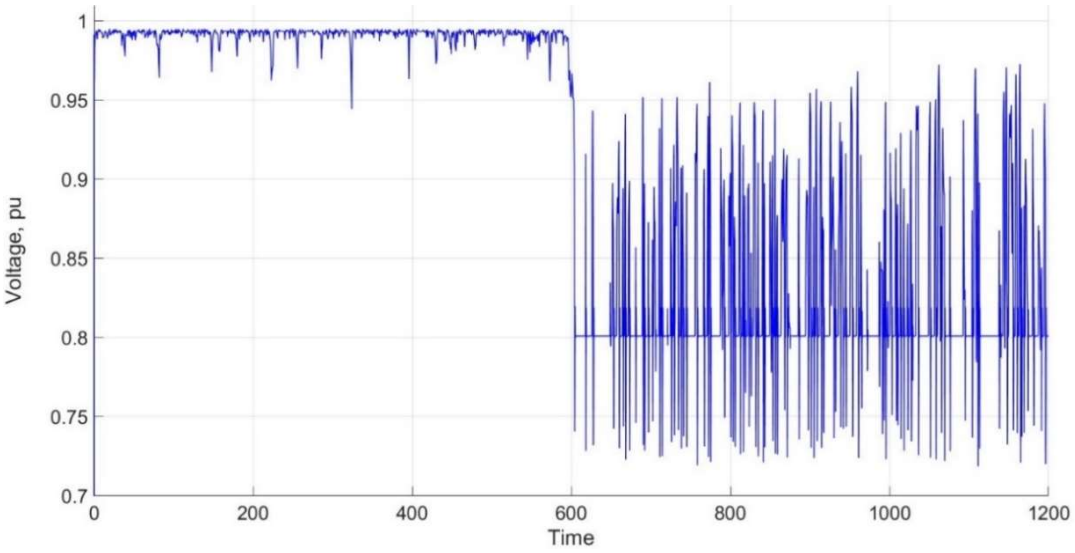

Figure 31 Maximum power value for small-signal case.

However, the wind turbine capacity value does not fit the voltage requirements after and during a fault because the recovered voltage value is smaller than 0.9 p.u. The result of the large disturbance test for the 465 MW turbine is attached in Appendix I. So, after several iteration steps, the maximum power, which satisfies all restrictions, is 381,9 MW, which is on average equal to 2,62 SCR. The voltage values during and after the fault are shown in Figure 32.

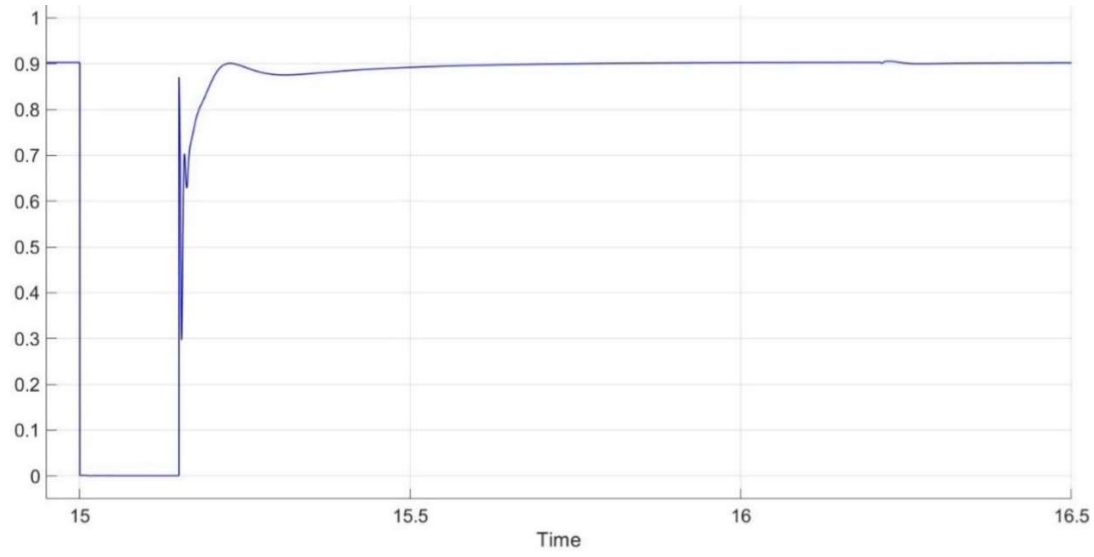

Figure 32 Short-circuit test of turbine maximum power.

The corresponding to this case voltage fluctuations at PCC during the small signal tests are shown in Appendix I.

Overall, this chapter has demonstrated the influence of the SCR ratio on a network and, considering the discussed example, the ability of the SCR index to be the criteria for limitation of the installed power in terms of stability, but with calculation for each particular case and with necessary consideration of the X/R ratio.

5. Simultaneity factor

This chapter contains definitions and application descriptions of a simultaneity factor for renewable energy sources, mainly electricity production from biomass, wind and solar power. Also, this chapter includes a study of relationships between the total installed capacity in a region and the simultaneity factor with its limits.

5.1 General concepts

The simultaneity factor is an index evaluated in a system for both the consumption and production sides. This phenomenon is called differently depending on the source and application: the factor of simultaneity, coincidence or diversity (Resch et al., 2017). Despite the diversity factor being defined as inverse to the simultaneity factor, the simultaneity factor is often called the diversity factor. The general formula is shown in Equation 22, according to the source (Resch et al., 2017).

$$\text{Simultainity factor} = \frac{\text{Total actual capacity}}{\text{Total installed capacity}} \quad (22)$$

The simultaneous factor evaluates how much available production or consumer capacity is loaded. Also, this value can be predictive and used in a system design. For example, there are French standard NFC14-100 for apartment houses without electrical heating, which sets the diversity factor depending on the number of planned consumers. So, according to the estimated consumption value for the apartment, it is possible to calculate the actual maximum demand for the house (Electrical Installation Wiki, n.d.). The French standard NFC14-100 is demonstrated in Table 9.

Table 9 French standard NFC14-100 (NFC, 2008)

Number of consumers	1 - 4	5 - 10	10 - 14	15 - 19	20 - 24
Simultaneity factor	1	0,78	0,63	0,53	0,49
Number of consumers	25 - 29	30 - 34	35 - 39	40 - 49	50+
Simultaneity factor	0,46	0,44	0,42	0,41	0,38

However, according to the chapter's aim, the simultaneity factor should be explored for the supply side. Especially, the factor is important for areas where variable renewable sources have implemented, because the maximum actual power significantly affects installed production power or auxiliary equipment rating in a system's nodes in regions (DNV GL, n.d.). For investigation of actual power production in a grid with renewable energy penetration, the most popular renewable sources in Germany were taken, such as wind, PV and biomass, which are the top 3 of installed capacity by the data from Chapter 3.

To demonstrate the real values of the simultaneity factor, the data are taken from the source (SMARD, 2023) and represent the sum of electricity produced from these 3 sources for each 15-minute interval for the entire 2017 year in the whole of Germany. These values are shown in Table 10.

Table 10 Simultaneity factor values in Germany.

Simultaneity factor	Biomass	PV	Wind	Total
Min	0,43	0,00	0,00	0,13
Average	0,54	0,10	0,21	0,25
Max	0,59	0,68	0,75	0,38

However, these values are calculated for a large region with huge total production capacities. Therefore, it is necessary to research the influence of scale on the production power and simultaneity factor.

5.2 Influence on actual power

Initially, the possible dependence between the simultaneity factor and the generated electricity on the selected region with a particular generation mix should be researched. So, calculations of correlation can estimate this. For this reason, the correlations between and within the selected sources are investigated below.

In general, there are three trends of correlation, each of which has its explanation described in the source (Widen, 2011). When correlation tends to 1, it enhances the overall electricity production growth, which is especially problematic during production peaks. The negative correlation, which tends to be -1, means that overall electricity

production is decreasing. The value of correlation about 0 demonstrates a lack of relationship.

The correlation data are shown in Table 11 and include values for small areas with low summarized installed capacity and large-scale areas with high total power. The small-scale values are represented by the area 100 square kilometers and 10 generators for each source type with a sum capacity of up to 17 MW (Nykamp, 2013). The large areas data is represented by the national scale regions, such as Germany and Sweden. Also, some values are calculated on the mentioned above data in RStudio software, and others are taken from the literature.

Table 11 Correlation values.

Correlation pairs	Small area	Source	Large are	Source
PV - Biomass	-0,050	(Nykamp, 2013)	0,033	Calculated
PV ´- Wind	-0,050	(Nykamp, 2013)	0,192; -0,2	Calculated; (Widen, 2011)
Wind - Biomass	-0,020	(Nykamp, 2013)	0,076	Calculated
Wind - Wind	0,850	(Nykamp, 2013)	0,150	(Widen, 2011)
PV - PV	0,950	(Nykamp, 2013)	0,800	(Widen, 2011)
Biomass - Biomass	0	(Nykamp, 2013)	-	-

Generally, electricity production from biomass sources only depends on inner parameters, such as productivity fluctuation and installed capacity (Nykamp, 2013). This conclusion is supported by the values from the table, where the correlation between biomass generators and the correlation between biomass and other sources for both observed scales are small and tend to be 0.

For PV and wind sources, the situation is more complicated. So, for the small-scale, correlations within the source types are high and tend to 1. However, the correlation between the PV and wind is approximately 0. This demonstrates that the electricity production from the Wind and PV power plants is almost summarized within each source,

but generally, the technologies are not dependent. Also, the lack of correlation between the sources allows them to simultaneously produce or not produce electricity, increasing the maximum possible value and reducing the minimum possible value of the actual power (Widen, 2011). Similarly, the range of the simultaneity factor values is expanded.

For large scale, the situation is different. The correlation within the photovoltaic source slightly decreased, compared to small-scale, while the correlation between wind generators dropped sharply. There is also a correlation between technologies of about 0.2, but the sign of the correlation differs depending on the source under consideration. So, adding PV capacity in a large region with just PV power will significantly increase simultaneous electricity producing or non-producing, while increasing wind power in analogical conditions will not have such a strong simultaneity effect. The correlation between the sources is small and indicates the coincidence or vice versa of the difference, depending on the source for the value, between the weather conditions for the periods under consideration (Widen, 2011). In general, this indicates that the simultaneity of the operation of sources over significant areas increases, which increases the overall average value and reduces the range of possible values of the actual power and, consequently, the average simultaneity factor.

So, as shown in the French standard example, the most exciting values for the simultaneity factor are its maximum values, which determine the installed power in a region under consideration. The edge values of the simultaneity factor for the Wind, PV and Biomass in the small-scale area are shown in more detail in the source (Resch et al., 2017). The values are shown in Table 12.

Table 12 Various limit values of the simultaneity factor (Resch et al., 2017).

	Biomass	PV	Wind
The maximum value of Simultaneity factor	1; 0,98	0,89; 0,95	1; 0,95
The minimum value of Simultaneity factor	0,6	0	0

The above conclusions about the simultaneity factor changes in dependence of the chosen area are confirmed, according to the values in Table 11 and Table 12.

It is also necessary to note the dependence of the maximum simultaneity factor on the number of considered generators. The source (Nykamp, 2013) contains a graph which shows the dependency of generators number by the sources on maximum produced power, which is the same as the maximum simultaneity factor. This graph is shown in Figure 33.

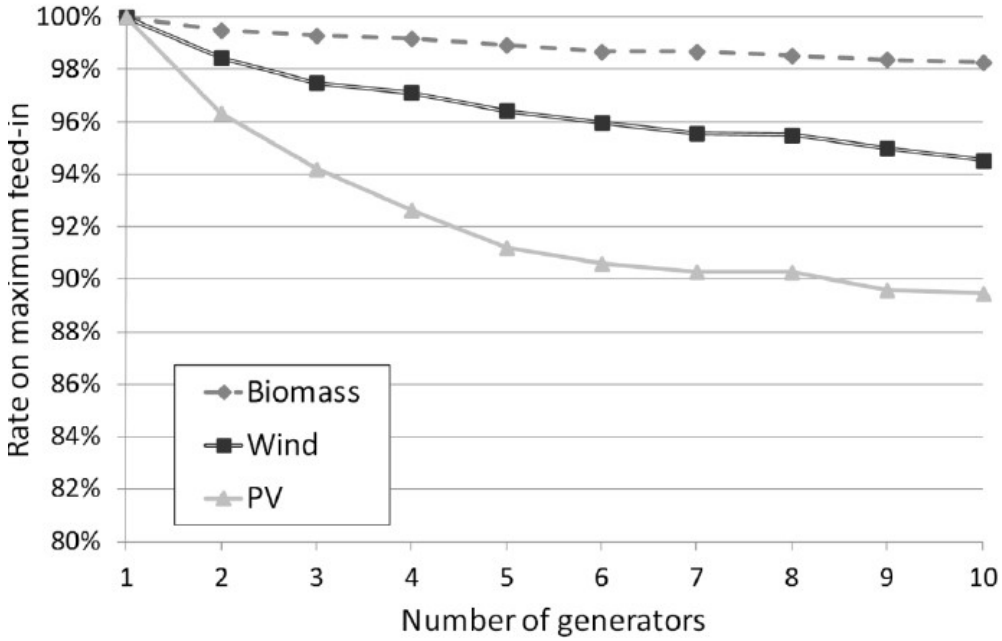

Figure 33 Diversity factor for different number of generators (Nykamp, 2013).

As can be seen from the Figure 33, increasing the observed number of production systems, in particular total installed capacity, decreases the maximum simultaneous actual power, and therefore decreases the maximum simultaneity factor (Nykamp, 2013).

5.3 Results

As was demonstrated in this chapter, the simultaneity factor is the forecasted value for planning and the calculated value for situation assessment. Ignoring the factor leads to unjustified expenses in scheme operation and construction because capacity installation planning and system stability tests are performed, considering limiting cases determined by the simultaneity factor (Electrical Installation Wiki, n.d.).

The main idea of the simultaneity factor is evaluating possible limits of actual production or consumption, which, in turn, defines the required installed power. Thus, the simultaneity factor is inextricably linked with the concept of installed power, and its calculation allows one to assess the situation in a region and adjust the installed power in the right direction. Besides this, based on the simultaneity factor, it is also possible to adjust the parts of a system, for example, in the case of evaluated overloading of the system nodes. This chapter showed how the type of renewable energy source, the scale of the area under consideration, and the total installed capacity within it affect the simultaneity factor. Also, as an example, the point of considering this factor was demonstrated in system stability tests in Chapters 3 and 4. In those cases, the simultaneity factor was assumed as 1, expressed in the choice of wind speed corresponding to the maximum turbine performance.

6. Overall conclusion

During the work, the main questions were successfully investigated. The penetration indices, namely the wind capacity penetration and wind energy penetration indices, have shown themselves as possible limiting criteria for installed capacity in a chosen region in terms of stability. This conclusion was made thanks to creating a simplified 3-phase electrical network model, including the variable load, the wind farm and the diesel generator, which unites conventional generation capacities and the exchange of electricity with other countries. Additionally, load variability is reached through the specially modelled block, and each main branch of the model contains the calculated transformer. As a result of tests, which are implemented according to the selected grid code, it was found that penetration indices are associated with system stability, and this allows them to be one of the limiting factors for installed power in the context of stability. Evaluation of the maximum share of the wind power index is also undoubtedly essential for the system because it allows one to limit the ratio of installed renewable energy in the region and prevents the system from wasting electricity, which does not allow unnecessary costs.

The short circuit ratio has been demonstrated as an important parameter of the network to which a wind farm is connected or planned to be connected. The index allows us to evaluate a system's stability and designate the maximum possible capacity, which can be connected to the network at a particular point of common coupling. The grid-connected wind farm model was developed and investigated to obtain this conclusion. This system consists of a wind farm line from the previous model and a current source with adjustable short-circuit power. As a result, the influence of different short-circuit ratio levels on grid stability and the index ability to estimate the maximum possible installed wind capacity were demonstrated. So, evaluating and considering the short-circuit ratio values is necessary because non-compliance with the recommendations would lead to disconnection from the network due to violations of the network operator's rules. Also, this section shows and tests the accompanying factor of the reactance to resistance ratio, which is also important and should also be considered with the investigation of short-circuit ratio values when connecting to the network.

The last item reviewed in this paper was the simultaneity factor considered for Germany's most popular renewable electricity sources, such as wind, solar and biomass plants. The existing values based on the available data and the influence exerted on this factor through the choice of region, particularly the generation mix, the total installed capacity or the number of generators, were shown for each type of generation source mentioned above. This index showed that it is inextricably linked to the installed capacity. Based on this factor and evaluation of related conditions, it is possible to set or adjust the maximum

value of installed capacity in a designed or operated system in a region under consideration.

During the study of the indices, in-depth work was also done to represent of existing examples and approximate the test conditions to real ones. So additional work includes:

- Creation of the wind speed generation program.
- Analysis of the different data, such as various parameters of the electrical market in Germany and the existing consumption profile.
- Investigation of the various standards and requirements to choosing the most optimal ones.

Of course, it is possible to go deeper into this topic by many parameters, such as more detailed modelling and analysis of more extensive and fresh data. However, the selected level allows one to get answers to the questions under study.

In conclusion, this work shown the possibility of using indices as a convenient tool to assess the stability degree and decide on the possible amount of installed capacity in terms of stability.

7. List of references

Ackermann, T. (ed) (2005) *Wind power in power systems*, Chichester, West Sussex, England, Hoboken, NJ, John Wiley.

Amprion GmbH (2015) *Calculation of transmission capacities between partner-grids* [Online], Dortmund, Amprion GmbH. Available at https://www.amprion.net/Dokumente/Strommarkt/Engpassmanagement/Kapazit%C3%A4tsmodelle/150520_capacity_calculation_scheme_amprion.pdf (Accessed 16 January 2023).

BDEW (2008) *Technische Richtlinie Erzeugungsanlagen am Mittelspannungsnetz* [Online], Berlin, Bundesverband der Energie und Wasserwirtschaft e. V. Available at https://www.bdew.de/media/documents/20080601_BDEW-Mittelspannungsrichtlinie.pdf (Accessed 12 May 2023).

BMWK (2023) *Grids and Grid Expansion: Grids and infrastructure* [Online], Berlin, Federal Ministry for Economic Affairs and Climate Action of Germany. Available at https://www.bmwk.de/Redaktion/EN/Artikel/Energy/electricity-grids-of-the-future-01.html (Accessed 3 March 2023).

Chapman, S. J. (2011) *Electric machinery fundamentals*, New York, McGraw-Hill.

Chouket, M. and Krichen, L. (eds) (2015) *Small signal modeling and stability analysis of wind turbine with PMSG connected to the grid* [Online]. Available at https://ieeexplore.ieee.org/document/7348167 (Accessed 17 March 2023).

Christiaan Zuur (n.d.) *System strength: Getting the grid sorted* [Online], Sydney, AEMC. Available at https://www.aemc.gov.au/strong-system-future-grid (Accessed 18 January 2023).

Clausen, N.-E. (2013) *Planning and development of wind farms: Environmental impact and grid connection.* [Online], Denmark, DTU Wind Energy (46). Available at https://orbit.dtu.dk/files/104234206/DTU_Wind_Energy_Report_I_46.pdf (Accessed 17 January 2023).

DNV GL (n.d.) *WindFarmer: Analyst User Guide* [Online], Norway, DNV GL. Available at https://dnvgldocs.azureedge.net/WindFarmer:%20Analyst_Latest/CalcRef/DesignTurbulence/designTurbulence.html.

Donohoe, P. (2013) *Fundamentals of Energy Systems* [Online], USA, Mississippi State University. Available at https://my.ece.msstate.edu/faculty/donohoe/ece3614three_phase_power.pdf (Accessed 20 April 2023).

Earnest, J. (2019) *Wind power technology*, India, PHI Learning.

Edrisian, A., Goudarzi, A. and Ebadian, M. (2014) 'Investigating the effect of high level of wind penetration on voltage stability by quasi-static time-domain simulation (QSTDS)', *International Journal of Renewable Energy Research*, vol. 4, no. 2 [Online]. Available at https://www.researchgate.net/publication/263355104_Investigating_the_effect_of_high_level_of_wind_penetration_on_voltage_stability_by_quasi-static_time-_domain_simulation_QSTDS (Accessed 1 April 2023).

Electrical Installation Wiki (n.d.) *General rules of electrical installation design: Power loading of an installation* [Online], France, Schneider Electric SE. Available at https://www.electrical-installation.org/enwiki/General_rules_of_electrical_installation_design (Accessed 19 May 2023).

ENTSO-E (2013) *Requirements for Grid Connection Applicable to all Generators* [Online], Belgium, ENTSO-E. Available at https://www.entsoe.eu/fileadmin/user_upload/_library/resources/RfG/130308_Final_Version_NC_RfG.pdf (Accessed 6 May 2023).

ENTSO-E (2023) *Transparency Platform* [Online], ENTSO-E. Available at https://transparency.entsoe.eu/ (Accessed 10 May 2023).

European Transmission System Operators (2001) *Definition of Transfer Capacities in liberalised Electricity Markets* [Online], Brussels, ETSO. Available at https://www.entsoe.eu/fileadmin/user_upload/_library/ntc/entsoe_transferCapacityDefinitions.pdf (Accessed 12 December 2022).

European Union (2018) *A European strategic long-term vision for a prosperous, modern, competitive and climate neutral economy* [Online], Brussels, European Union. Available at https://ec.europa.eu/commission/presscorner/detail/en/IP_18_6543 (Accessed 11 February 2023).

Global Wind Atlas 3.0 (2023) *Wind Speed data* [Online], Technical University of Denmark. Available at https://globalwindatlas.info/ (Accessed 22 January 2023).

Golieva, A. (2015) *Low Short-Circuit Ratio Connection of Wind Power Plants*, Master of Science Thesis, Norway, Norwegian University of Science and Technology [Online]. Available at https://repository.tudelft.nl/islandora/object/uuid:ebae4f63-7dee-4091-876e-5ff46f15c6d0/datastream/OBJ/download (Accessed 20 May 2023).

Hannesdottir, A., Kelly, M. and Dimitrov, N. (2018) *Extreme fluctuations of wind speed for a coastal/offshore climate: statistics and impact on wind turbine loads* [Online], Norway, DTU Wind Energy. Available at https://www.researchgate.net/publication/

323320474_Extreme_fluctuations_of_wind_speed_for_a_coastaloffshore_climate_statistics_and_impact_on_wind_turbine_loads (Accessed 18 April 2023).

Hatziargyriou, N., Milanovic, J., Rahmann, C., Ajjarapu, V., Canizares, C., Erlich, I., Hill, D., Hiskens, I., Kamwa, I., Pal, B., Pourbeik, P., Sanchez-Gasca, J., Stankovic, A., van Cutsem, T., Vittal, V. and Vournas, C. (2021) 'Definition and Classification of Power System Stability – Revisited & Extended', *IEEE Transactions on Power Systems*, vol. 36, no. 4, pp. 3271–3281 [Online]. DOI: 10.1109/TPWRS.2020.3041774 (Accessed 11 May 2023).

IEA (2022) *Renewables Data Explorer* [Online], Paris, IEA. Available at https://www.iea.org/data-and-statistics/data-tools/renewables-data-explorer (Accessed 29 December 2022).

IEC (2001) *IEC 61400-21:2001: Measurement and Assessment of Power Quality Characteristics of Grid Connected Wind Turbines*, Geneva, Switzerland: International Electrotechnical Commission.

IEC (2005) *IEC 61400-1: Wind turbines, Part 1: Design requirements*: IEC [Online]. Available at https://webstore.iec.ch/publication/5426 (Accessed 11 January 2023).

IEEE (1992) *IEEE 421.5-1992: Recommended Practice for Excitation System Models for Power System Stability Studies*: IEEE [Online]. Available at https://ieeexplore.ieee.org/servlet/opac?punumber=2901 (Accessed 12 March 2023).

IEEE (2020) *IEEE 1110-2019: Guide for Synchronous Generator Modeling Practices and Parameter Verification with Applications in Power System Stability Analyses*: IEEE [Online]. Available at https://ieeexplore.ieee.org/servlet/opac?punumber=9020272 (Accessed 12 February 2023).

Impram, S., Varbak Nese, S. and Oral, B. (2020) 'Challenges of renewable energy penetration on power system flexibility: A survey', *Energy Strategy Reviews*, vol. 31 [Online]. DOI: 10.1016/j.esr.2020.100539 (Accessed 17 April 2023).

Kumari, N., Singh, S., Kumari, R., Patel, R. and Xalxo, N. (2016) 'Power System Faults: A Review', *International jornal of engineering reseach & technology (IJERT)*, vol. 4, no. 2 [Online]. Available at https://www.ijert.org/power-system-faults-a-review (Accessed 19 March 2023).

Lackovic, V. (2023) *Power System Transient Stability Study Fundamentals: Cource document* [Online], CEDengineering. Available at https://www.cedengineering.com/courses/power-system-transient-stability-study-fundamentals (Accessed 25 March 2023).

Lei, C., Wu, Y., Huang, Y., Liang, Y., Nie, J., Tang, M., Yi, X. and Luo, Y. (2022) 'Research on Maximum Penetration Ratio of Wind Power under the Voltage Stability Margin Constraint', *Sustainability*, vol. 14, no. 12 [Online]. DOI: 10.3390/su14127217 (Accessed 29 April 2023).

Leila, M., Mounira, M., Amel, O. and Salah, S. (2017) 'Modelling and control of wind turbine doubly fed induction generator with MATLAB simulink', *Global Journal of Computer Sciences: Theory and Research*, vol. 7, no. 2, pp. 77–91 [Online]. DOI: 10.18844/gjcs.v7i2.2714.

Liu, J., Hu, H., Yu, S. S. and Trinh, H. (2023) 'Virtual Power Plant with Renewable Energy Sources and Energy Storage Systems for Sustainable Power Grid-Formation, Control Techniques and Demand Response', *Energies*, vol. 16, no. 9 [Online]. DOI: 10.3390/en16093705 (Accessed 1 February 2023).

Londero, R. R., Affonso, C. d. M. and Vieira, J. P. A. (2015) 'Long-Term Voltage Stability Analysis of Variable Speed Wind Generators', *IEEE Transactions on Power Systems*, vol. 30, no. 1, pp. 439–447 [Online]. DOI: 10.1109/TPWRS.2014.2322258 (Accessed 11 April 2023).

Meegahapola, L. and Flynn, D. (2010) 'Impact on transient and frequency stability for a power system at very high wind penetration', *IEEE PES General Meeting.* Minneapolis, MN, 25.07.2010 - 29.07.2010, IEEE, pp. 1–8.

Meegahapola, L. and Littler, T. (2015) 'Characterisation of large disturbance rotor angle and voltage stability in interconnected power networks with distributed wind generation', *IET Renewable Power Generation*, vol. 9, no. 3, pp. 272–283 [Online]. DOI: 10.1049/iet-rpg.2013.0406 (Accessed 9 March 2023).

Milligan, M., Donohoo, P., Lew, D., Ela, E., Kirby, B., Holttinen, H., Lannoye, E., Flynn, D., O'Malley, M., Miller, N., Eriksen, P. B., Gottig, A., Rawn, B., Gibescu, M., Lazaro, E. G., Robitaille, A. and Kamwa, I. (eds) (2010) *Operating Reserves and Wind Power Integration: An International Comparison* [Online], United States. Available at https://www.osti.gov/servlets/purl/992809 (Accessed 12 December 2022).

Navarro, D. (2021a) *Grid Connection*, Ingolstadt.

Navarro, D. (2021b) *Site-Assessment*, Ingolstadt.

NFC (2008) *NFC 14-100 : 2008: LOW-VOLTAGE MAINS INSTALLATIONS*, France: Association Francaise de Normalisation [Online]. Available at https://shop.standards.ie/en-ie/standards/nfc-14-100-2008-amd-3-2016-47969_saig_afnor_afnor_104618/ (Accessed 19 March 2023).

Nykamp, S. (2013) *Integrating renewables in distribution grids: Storage, regulation and the interactions of different stakeholders in future grids* [Online], Enschede, University of Twente. Available at https://research.utwente.nl/en/publications/integrating-renewables-in-distribution-grids-storage-regulation-a (Accessed 6 April 2023).

Okedu, K. (2022) 'Improving the Performance of PMSG Wind Turbines During Grid Fault Considering Different Strategies of Fault Current Limiters', *Frontiers in Energy Research*, vol. 10 [Online]. DOI: 10.3389/fenrg.2022.909044 (Accessed 12 February 2023).

Open Power System Data (2020) *Data Package Household Data. Version 2020-04-15* [Online]. Available at https://data.open-power-system-data.org/household_data/ (Accessed 28 April 2023).

Perelmuter, V. (2017) *Electrotechnical systems: Simulation with Simulink and SimPowerSystems*, Boca Raton, CRC Press.

Reginatto, R. and Rocha, C. (2009) *Minimum Short-Circuit Ratios for Grid Interconnection of Wind Farms with Induction Generators* [Online], Brazil, CLAGTEE. Available at https://www.researchgate.net/publication/236661861_Minimum_Short-Circuit_Ratios_for_Grid_Interconnection_of_Wind_Farms_with_Induction_Generators (Accessed 17 April 2023).

Resch, M., Bühler, J., Klausen, M. and Sumper, A. (2017) 'Impact of operation strategies of large scale battery systems on distribution grid planning in Germany', *Renewable and Sustainable Energy Reviews*, vol. 74, pp. 1042–1063 [Online]. DOI: 10.1016/j.rser.2017.02.075 (Accessed 11 April 2023).

Sajadi, A., Zhao, S., Clark, K. and Loparo, K. (2019) 'Small-Signal Stability Analysis of Large-Scale Power Systems in Response to Variability of Offshore Wind Power Plants', *IEEE Systems Journal*, vol. 13, no. 3, pp. 3070–3079 [Online]. DOI: 10.1109/JSYST.2018.2885302 (Accessed 7 April 2023).

Shi, L. B., Wang, C., Yao, L. Z., Wang, L. M. and Ni, Y. X. (2011) 'Analysis of impact of grid-connected wind power on small signal stability', *Wind Energy*, vol. 14, no. 4, pp. 517–537 [Online]. DOI: 10.1002/we.440 (Accessed 12 January 2023).

Shipp, D. and Angelini, F. (eds) (1988) *Characteristics of different power systems grounding techniques: fact and fiction* [Online], Pittsburgh. Available at https://ieeexplore.ieee.org/document/25261 (Accessed 13 May 2023).

Simpson, J. and Loth, E. (2022) ‘Super-rated operational concept for increased wind turbine power with energy storage’, *Energy Conversion and Management: X*, vol. 14, p. 100194 [Online]. DOI: 10.1016/j.ecmx.2022.100194 (Accessed 5 March 2023).

SMARD (2021) *User guide* [Online], Bonn, Germany, Bundesnetzagentur. Available at https://www.smard.de/resource/blob/205652/63fcff2c9813096fa2229d769da164ef/smard-user-guide-09-2021-data.pdf (Accessed 21 February 2023).

SMARD (2023) *German electricity market data* [Online], Bundesnetzagentur. Available at https://www.smard.de/ (Accessed 3 April 2023).

Swe, O. (2020) ‘Modelling and Simulation for Small Signal Stability of Multi-machine Power System under Various Disturbance Conditions’, *Journal on Advanced Research in Electrical Engineering*, vol. 4, no. 1 [Online]. DOI: 10.12962/j25796216.v4.i1.103 (Accessed 12 May 2023).

Tande, J. O. G. (2000) ‘Exploitation of wind-energy resources in proximity to weak electric grids’, *Applied Energy*, vol. 65, 1-4, pp. 395–401 [Online]. DOI: 10.1016/S0306-2619(99)00098-7 (Accessed 1 February 2023).

The MathWorks Inc. (2023a) *24-hour Simulation of a Vehicle-to-Grid (V2G) System* [Online], Natick, Massachusetts, United States, The MathWorks Inc. Available at https://de.mathworks.com/help/sps/ug/24-hour-simulation-of-a-vehicle-to-grid-v2g-system.html (Accessed 17 April 2023).

The MathWorks Inc. (2023b) *Excitation System: Documentation* [Online], Natick, Massachusetts, United States, The MathWorks Inc. Available at https://de.mathworks.com/help/sps/powersys/ref/excitationsystem.html (Accessed 17 April 2023).

The MathWorks Inc. (2023c) *Simplified Synchronous Machine: Documentation* [Online], Natick, Massachusetts, United States, The MathWorks Inc. Available at https://de.mathworks.com/help/sps/powersys/ref/simplifiedsynchronousmachine.html (Accessed 16 April 2023).

The MathWorks Inc. (2023d) *State-Space block: Documentation* [Online], Natick, Massachusetts, United States, The MathWorks Inc. Available at https://de.mathworks.com/help/simulink/slref/statespace.html (Accessed 17 April 2023).

The MathWorks Inc. (2023e) *Synchronous Machine pu Standard: Documentation* [Online], Natick, Massachusetts, United States, The MathWorks Inc. Available at https://de.mathworks.com/help/sps/powersys/ref/synchronousmachinepustandard.html (Accessed 17 April 2023).

The MathWorks Inc. (2023f) *Three-Phase Dynamic Load: Documentation* [Online], Natick, Massachusetts, United States, The MathWorks Inc. Available at https://de.mathworks.com/help/sps/powersys/ref/threephasedynamicload.html (Accessed 12 March 2023).

The MathWorks Inc. (2023g) *Three-phase source with internal R-L impedance: Documentation* [Online], Natick, Massachusetts, United States, The MathWorks Inc. Available at https://de.mathworks.com/help/sps/powersys/ref/threephasesource.html.

The MathWorks Inc. (2023h) *Wind Farm (IG)* [Online], Natick, Massachusetts, United States, The MathWorks Inc. Available at https://de.mathworks.com/help/sps/ug/wind-farm-ig.html (Accessed 15 May 2023).

The MathWorks Inc. (2023i) *Wind Turbine Doubly-Fed Induction Generator (Phasor Type): Documentation* [Online], Natick, Massachusetts, United States, The MathWorks Inc. Available at https://de.mathworks.com/help/sps/powersys/ref/windturbinedoublyfedinductiongeneratorphasortype.html (Accessed 11 May 2023).

Tikhomirov, P. (1986) *Calculation of transformers*, Moscow, Energoatomizda.

Toma, L., Bompard, E. and Mazza, A. (2021) 'Modal analysis', in *Converter-Based Dynamics and Control of Modern Power Systems,* Elsevier, pp. 67–89.

VDE (2018) *VDE-AR-N 4110: Technical Connection Rules for Medium-Voltage*, Berlin [Online]. Available at https://www.vde.com/en/fnn/topics/technical-connection-rules/tcr-for-medium-voltage (Accessed 12 April 2023).

Vilmann, B., Randewijk, P. J., Jóhannsson, H., Hjerrild, J. and Khalil, A. (2023) 'Frequency and Voltage Compliance Capabilities of Grid-Forming Wind Turbines in Offshore Wind Farms in Weak AC Grids', *Electronics*, vol. 12, no. 5 [Online]. DOI: 10.3390/electronics12051114 (Accessed 11 April 2023).

Widen, J. (2011) 'Correlations Between Large-Scale Solar and Wind Power in a Future Scenario for Sweden', *IEEE Transactions on Sustainable Energy*, vol. 2, no. 2, pp. 177–184 [Online]. DOI: 10.1109/TSTE.2010.2101620 (Accessed 18 March 2023).

Xu, Z., Zhang, N., Zhang, Z. and Huang, Y. (2023) 'The Definition of Power Grid Strength and Its Calculation Methods for Power Systems with High Proportion Nonsynchronous-Machine Sources', *Energies*, vol. 16, no. 4, p. 1842 [Online]. DOI: 10.3390/en16041842 (Accessed 29 April 2023).

Yadav, V. and Saravanan, B. (2022) ‘Technical advances and stability analysis in wind-penetrated power generation systems—A review’, *Frontiers in Energy Research*, vol. 10 [Online]. DOI: 10.3389/fenrg.2022.1091512 (Accessed 11 June 2023).

8. Appendices

Appendix A

Table - Technical Interconnection Regulations (ENTSO-E, 2013) and (Ackermann, 2005).

<table>
<tr><th colspan="2">Active power</th></tr>
<tr><td>Value characteristic:
1 min. average</td><td>Power in any time ≤ Registered capacity
Power reduction ≥ 10% of registered capacity
Power increase ≤ 10% of registered capacity</td></tr>
<tr><th colspan="2">Startup and Shutdown</th></tr>
<tr><td colspan="2">According with requirements regarding active power change and voltage quality</td></tr>
<tr><th colspan="2">Frequency</th></tr>
<tr><td>Value characteristic:
10 min. average</td><td>Normal operation conditions: 50Hz ± 1%
• If frequency exceed 51,5 Hz or below 47,5 Hz, the generator should be disconnected immediately.
• If the generator frequency is between 50,5 Hz and 51,5 Hz, power should be decreased by 4% per 0.1 Hz of excess.
• If the generator frequency is between 47,5 Hz and 49,5 Hz, power should be reduced by 1% per 0.1 Hz of excess.</td></tr>
<tr><th colspan="2">Reactive power</th></tr>
<tr><td colspan="2">• Power Factor (PF) ≥ 0,925 in generating reactive power mode.
• PF ≥ 0,95 in absorbing reactive power mode.
• This regulation is presented in a table Reactive power requirements below</td></tr>
<tr><th colspan="2">Voltage quality</th></tr>
<tr><td>Value for variations:
per 10 min.</td><td>Voltage magnitude variation: ±10% for 95% of week</td></tr>
</table>

<table>
<tr><td>Value for variations: per 10 min.</td><td colspan="2">Voltage magnitude variation: ±10% for 95% of week</td></tr>
<tr><td>Value for voltage changes: max. value per 1 min.</td><td colspan="2">Rapid voltage changes: ≤ 2% of nominal voltage</td></tr>
<tr><td>Value for flicker: weighted average value for 2 hours</td><td colspan="2">Voltage flicker: P_{lt} ≤ 0,46</td></tr>
<tr><td colspan="2">Harmonic critical values [A/MVA],
n < 26 and n is odd:
• D_n < 0,01–0,115, 10 kV
• D_n < 0,005–0,058, 20 kV</td><td>Harmonic critical values [A/MVA],
n is even or n > 26:
• D_n < 0,06/n, 10 kV
• D_n < 0,03/n, 20 kV</td></tr>
<tr><td colspan="3">Voltage frames during and after the fault:
• If the voltage drops below 20% of the nominal, the generator will be disconnected after 0,7 s.
• If the voltage drops below 80% of the nominal, the generator will be disconnected after 3 s.

Voltage operational frames:
• If the voltage drops below 90% of the nominal, the generator will be disconnected after 60 s.
• If the voltage drops below 80% of the nominal, the generator will be disconnected after 3 - 5 s.
• If the voltage exceeds 120% of the nominal, the generator will be disconnected after 0,2 s.

Voltage normal range:
90% ≤ V ≤ 110%</td></tr>
</table>

Where rapid voltage changes is a single rapid change (increase/decrease) of voltage (RMS), P_{lt} is the weighted average flicker emission, and D_n is the harmonic interference of each harmonic wave n, which is an positive integer (Ackermann, 2005).

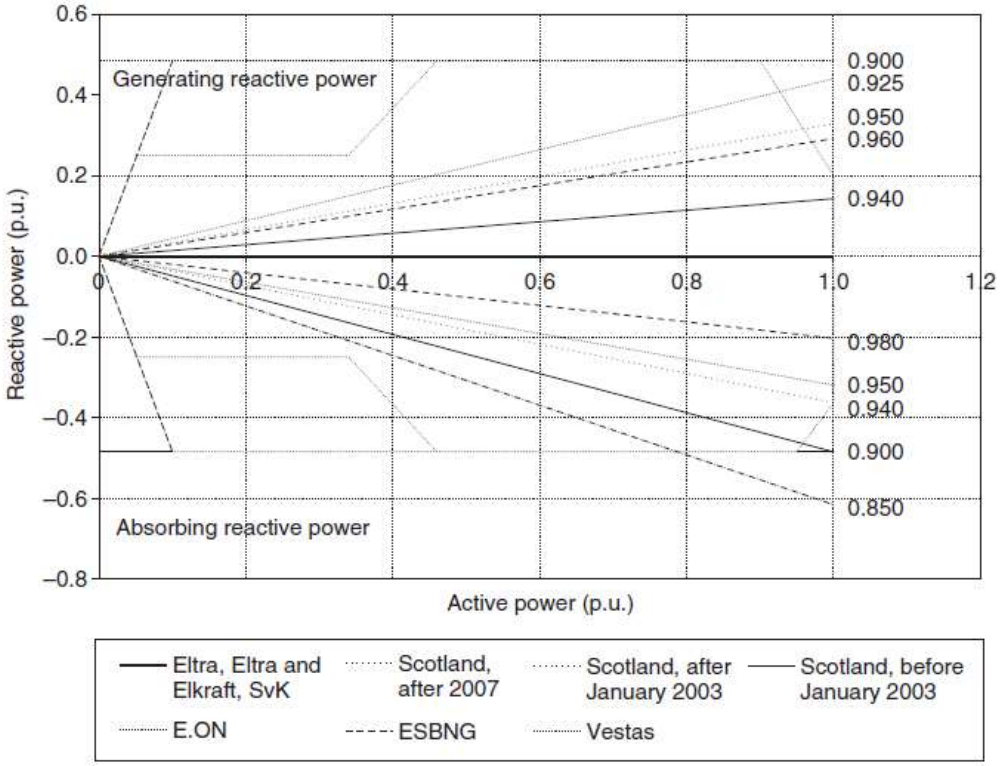

Figure. Reactive power requirements (Ackermann, 2005).

Table. Time-voltage requirements during and after fault (ENTSO-E, 2013).

Voltage parameters, p.u.		Time parameters, s	
V ret	0,05 – 0,3	T clear	0,14 – 0,25
V clear	0,7 – 0, 9	T rec1	T clear
V rec1	V clear	T rec 2	T rec1 – 0,7
V rec2	0,85 – 0,9 and ≥ V clear	T rec 3	T rec 2 – 1,5

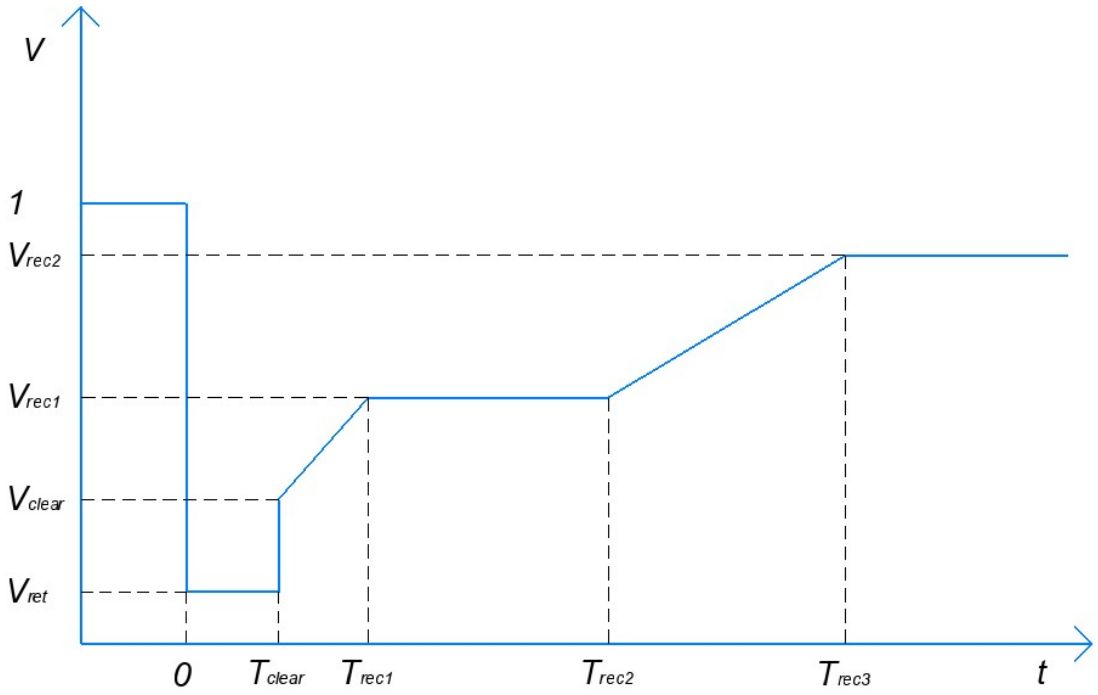

Figure. Time-voltage requirements during and after fault. Adopted from (ENTSO-E, 2013).

Appendix B

Wind speed generation code in R language, written in RStudio software

```
library("mixdist")
library("stats")

#Average wind speed for 2022 in Germany at high 150m and 100m at 100% area
# According to the site "globalwindatlas"
V.ave150 = 7.82
V.ave100 = 6.77

#Turbulent Classes at 15m/s
I1 = 0.12
I2 = 0.14
I3 = 0.16

MVdata <-V.ave100  #1st accepted value and setting array for 10 min. values
data = c() #2nd empty array for 1 sec. values
sdI <- (4.5)^(0.5) #Standard deviation for 1s time frame

#Generation body
for(i in 1:2) {

  #Evaluation of standard deviation according to the IEC 61400-1 standard,
  #5,6 is constant for assumed rotor diameter, which is bigger than 50 m.
  sd <- I1*(0.75*MVdata[i]+5.6)

  #Finding the Weibull distribution parameters (1st array), in particular
  #shape and scale, based on calculated standard deviation
  #and mean wind speed (previous 10min value)
  ParMV <- mixdist::weibullpar(MVdata[i], sd)

  #Evaluation of the next value in the 10 min array
  MVdata[i+1] <- rweibull(1,ParMV$shape,ParMV$scale)

  #Finding the Weibull distribution parameters (2nd array),in particular
  #shape and scale, based on calculated standard deviation and mean
  #wind speed (10 min value corresponded for this interval)
  Par <- mixdist::weibullpar(MVdata[i], sdI)

  # Generating array of each 1 second values
  data <- append(data, rweibull(600,Par$shape,Par$scale))
}
```

Appendix C

Table. Annual data of additional parameters.

Calc before	2015	2016	2017	2018	2019	2020	2021	2022
Average provided balancing energy MWh in 1h	358,89	368,52	356,16	386,99	416,72	360,64	342,27	399,94
Sum Renewable production TWh	112,06	111,91	138,49	149,57	166,18	175,81	160,03	180,60
Sum Consumption TWh	500,22	503,09	505,67	509,16	497,29	485,29	504,52	483,66
Avg. Transfer energy MWh	358,80	368,31	356,17	386,96	416,94	360,86	342,27	401,26

Appendix D

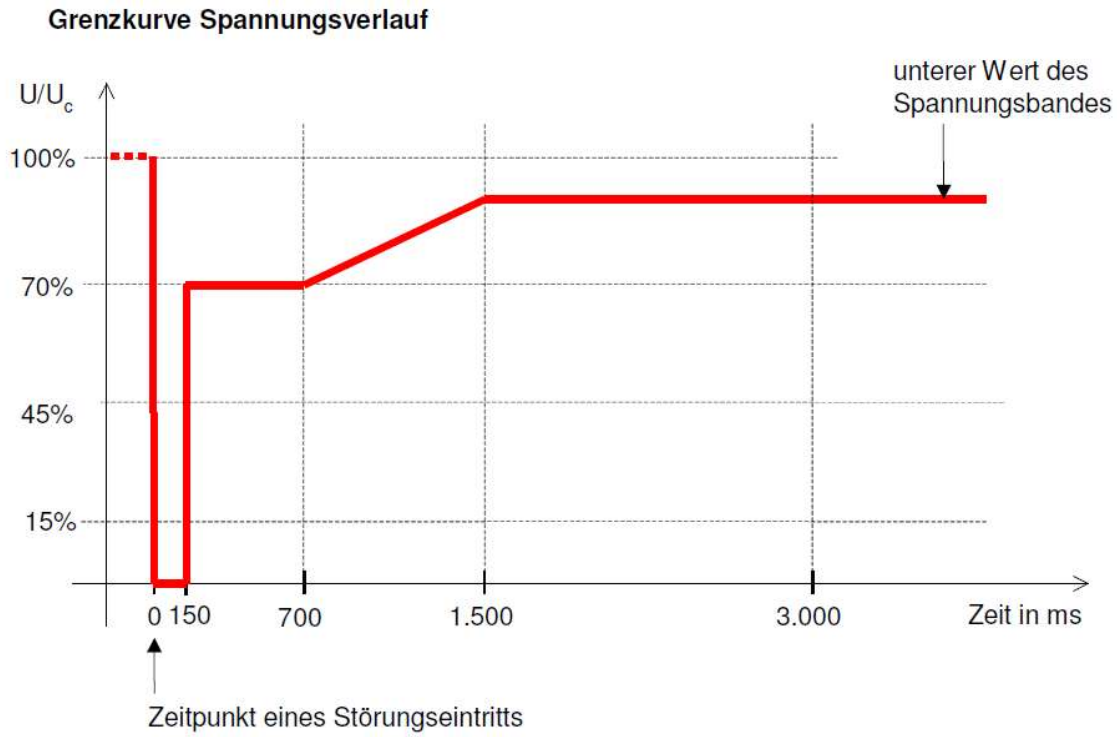

Figure. Time-voltage limits for directly connected synchronous generators (BDEW, 2008).

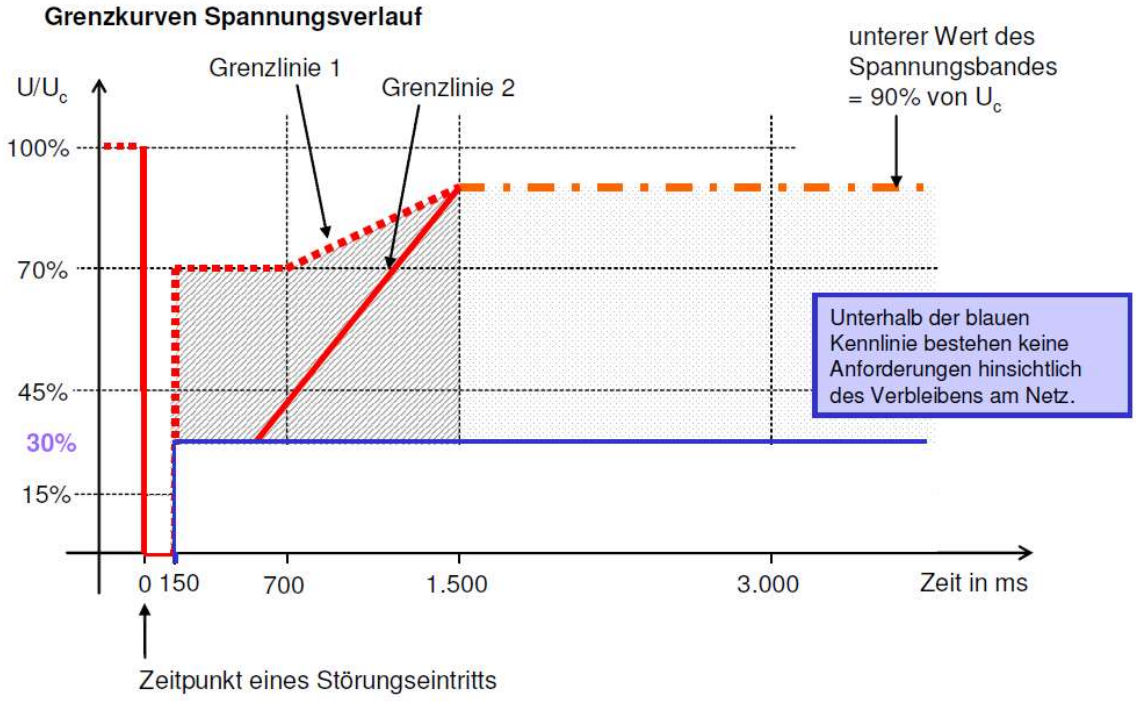

Figure. Time-Voltage limits for other type connections. (BDEW, 2008)

Below the blue curve there are no requirements for staying connected.

Appendix E

Table. Wind turbine data.

Generator	
Generator rating, MVA	2,1
L-L voltage, V (RMS)	575
Frequency, Hz	50
Stator resistance, in p.u. of the generator rating	0,005
Leakage inductance, in p.u. of the generator rating	0,13
Rotor resistance, p.u. of the generator rating	0,004
Rotor leakage inductance, p.u. of the generator rating	0,17
Magnetizing inductance, p.u. of the generator rating	7,02
Inertia constant, s	1
Viscous friction factor, p.u. of the generator rating	0
Number of pole pairs	3
Initial conditions	0
Turbine	
Nominal mechanical power, MW	2
Tracking characteristic speeds in p.u. of synchronous speed	0,65; 0,69; 1,2; 1,31
Power at point C, p.u./mechanical power	0,8
Wind speed at point C, m/s	11

Pitch angle controller gain	15
Maximum pitch angle, degrees	30
Maximum rate of change of pitch angle, deg/s	5
Converter	
Converter maximum power, p.u. of nominal power	0,3
GS. inductive coupling, p.u. of generator rating	0,6
GS. resistance, p.u. of generator rating	0,1
Initial positive phasor current of coupled inductor in form of magnitude and phase, p.u. and degrees	0; 90
Nominal DC bus voltage, V	1150
DC bus capacitor, F	1e-2
Control	
Regulation mode	Voltage regulation
Reference voltage, p.u. of nominal voltage	1
Reference reactive current of GS. converter, p.u.	0
Grid voltage regulator gains	1,25; 300
Droop reactance, p.u./nominal power	0,02
Power regulator gains	1; 100
DC bus voltage regulator gains	0,002; 0,05
GS. converter current of controller gains	1; 100

RS. converter current of controller gains	0,3; 8
Max. change rate of grid voltage	100
Max. change rate of power	1
Max. change rate of converter currents	200

Figure. RS. converter control scheme (The MathWorks Inc., 2023i).

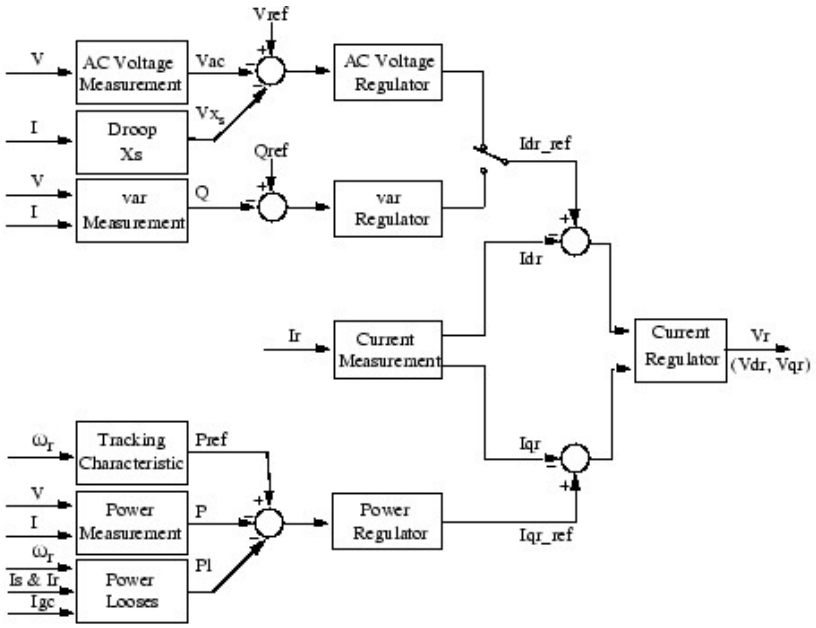

Figure. GS. converter control scheme (The MathWorks Inc., 2023i).

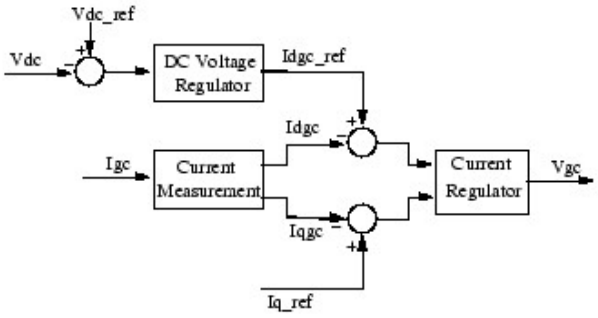

Figure. Pitch angle control scheme (The MathWorks Inc., 2023i).

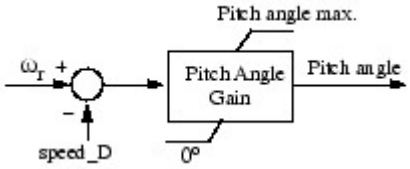

Table. Manufacturer's transformer data (Tikhomirov, 1986).

Parameter	**Value**
Nominal power, kVA	2500
Voltage rating	Up to 35kV
The impedance of the transformer, %	6,5
No-load current, %	1,0
No-load losses, W	3900
Short-circuit losses, W	26000

Table. Parameters of additional load block.

Configuration	Y-grounded
P-P voltage, V (RMS)	575
Frequency, Hz	50
Active power, W	1e3
Inductive reactive power, VAr	0
Capacitive reactive power, VAr	0
Load type	Z constant

Table. Wind turbine branch transformer.

Configuration	
Connections	Y-Y
Core type	3 single phase
Parameters	
Units	p.u.
Nominal power and frequency, VA and Hz	2500; 50
Winding 1: Voltage, Resistance and Inductance; (V in ph-ph RMS), p.u. and p.u.	575; 0,0104; 0,0325
Winding 2: Voltage, Resistance and Inductance; (V in ph-ph RMS), p.u. and p.u.	33e3; 0,0104; 0,0325
Magnetization resistance, p.u.	641
Magnetization inductance, p.u.	98,8

Appendix F

According to the source (The MathWorks Inc., 2023e), the generator is represented by state-space of 6th order. This block includes modelling the stator, field, and damper windings. Stator winding is Y connection to a neutral. Rotor parameters are defined based on the stator values.

Figure. The electrical scheme of synchronous generator (The MathWorks Inc., 2023e).

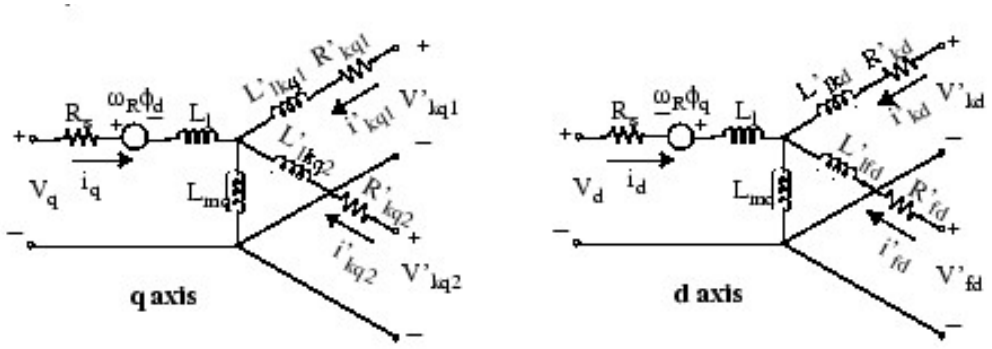

Where L is leakage inductance, L_m is magnetizing inductance, f is number of field windings, k is number of damped windings.

Figure. The mechanical scheme of synchronous generator (The MathWorks Inc., 2023c)

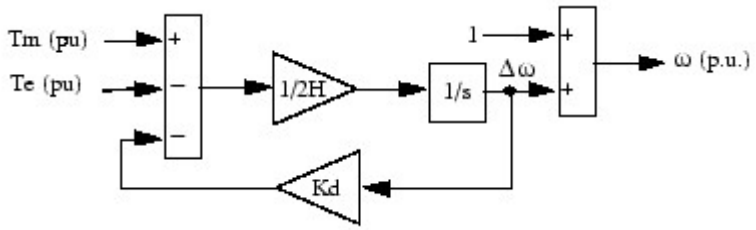

2 main equations describing mechanical part of the transformer according to the source (The MathWorks Inc., 2023c)

$$\Delta\omega(t) = \frac{\int_o^t (Tm - Te) - Kd\Delta\omega(t)dt}{2 * H} \qquad (a)$$

$$\omega(t) = \Delta\omega(t) + \omega_0 \qquad (b)$$

Where $\Delta\omega$ - Speed difference, H – inertia constant, $\Delta\omega$ - mechanical torque, T_e - electromagnetic torque, ω – rotor speed, ω_0 - working speed, K_d - damping coefficient (The MathWorks Inc., 2023e)

Figure. Standard excitation system (IEEE, 1992).

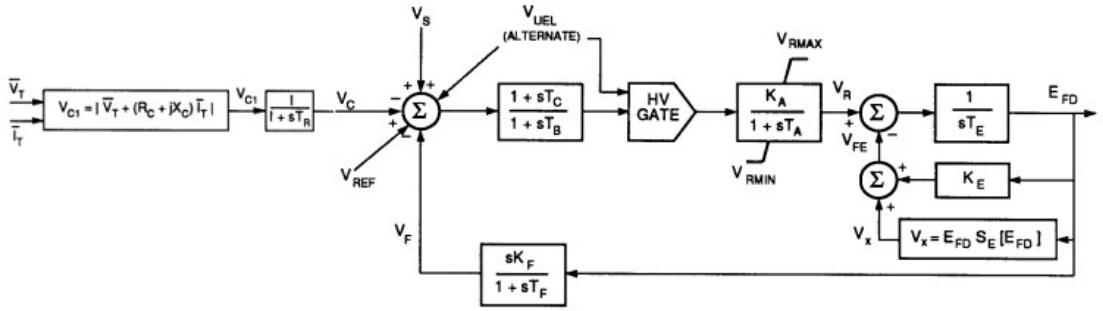

Figure. Simulink excitation system (The MathWorks Inc., 2023b).

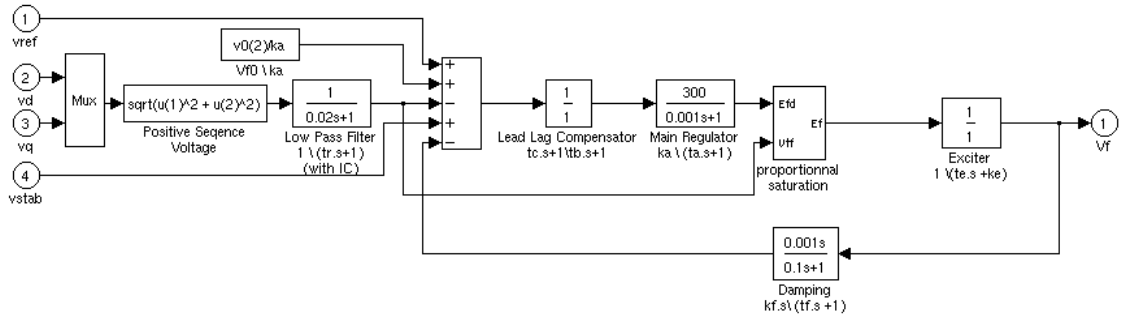

Table. Governor block data (Perelmuter, 2017).

Controller block		Servomotor block	
T3	5	Initial value	0,5
To	0,02	Upper limit	1
ζ	0,3	Lover limit	0
K	20	Delay block	
-		Time delay	0.1

Appendix G

Figure. Dynamic load block parameters.

L-L nominal voltage, kV	33
Frequency, Hz	50
Initial voltage represented in magnitude and phase, p.u.	0,8; 0
Active and reactive power corresponding to initial voltage, MW and VAr	2,7; 0
Coefficients of the described equations, np, nq	1,1
Time constants of the described equations	0; 0; 0; 0
Min. voltage, p.u.	0,8
Filtering time constant	1e-4

Derivation of main equations used for defining the consumption:

$$V_a = \frac{(V_{ab} - a^2 * V_{bc})}{3} \quad (18)$$

$$a^2 = e^{-j*\frac{2*\pi}{3}} \quad (19)$$

So, a is a phase angle between 2 phases, which equal to 120 degrees. Thus, Multiplication of value on "a" shift to 120 degrees and on "a^2" shift to -120 degrees. The equation of "a" is shown below.

$$a = e^{j*\frac{2*\pi}{3}} (a)$$

Thus $a^2 * V_{bc}$ should be equal to V_{ca}. Derivation of it is shown below, taking into account equations from the sources (Chapman, 2011) and (Donohoe, 2013) and that balanced system in positive sequence order.

$$a^2 = e^{-j*\frac{2*\pi}{3}} = \cos(120) - j * \sin(120) = -\frac{1}{2} - j * \frac{\sqrt[2]{3}}{2}$$

$$a^2 * V_{bc} = \sqrt[2]{3} * V_{rms} * \left(-2 * j * \frac{\sqrt[2]{3}}{2}\right) * \left(-\frac{1}{2} - j * \frac{\sqrt[2]{3}}{2}\right) = 3 * V_{rms} * \left(\frac{-\sqrt[2]{3} + j}{2}\right)$$
$$= V_{ca}$$

The next step is deviation of the overall equation, in particular that $\frac{(V_{ab} - V_{ca})}{3}$ equals to V_a.

$$\frac{(V_{ab} - V_{ca})}{3} = \frac{V_{rms}}{\sqrt[2]{3}} * \left(\left(\frac{\sqrt[2]{3} + j}{2}\right) - \left(\frac{-\sqrt[2]{3} + j}{2}\right)\right) = \frac{V_{rms}}{\sqrt[2]{3}} * \left(\frac{\sqrt[2]{3} * 2}{2}\right) = V_{rms} = V_a$$

Thus, according to the formula obtained, the voltage of phase A is evaluated. Then, according to the scheme and block of the controlled current source, is induced a linear voltage converting into a phase current. (According to measurement blocks, peak values should be input)

Table. State-space block values.

A	-10
B	1
C	10
D	0
Initial condition:	0

The equations form of the state-space blocks (The MathWorks Inc., 2023d):

$$\dot{x} = \mathrm{Ax} + \mathrm{Bu}\ (\mathrm{b})$$

$$y = \mathrm{Cx} + \mathrm{Du}\ (\mathrm{c})$$

$$x_{t=t_0} = x_0\ (\mathrm{d})$$

Where $\mathrm{A}, \mathrm{B}, \mathrm{C}, \mathrm{D}$, are constant, x is a state vector, u is input, y is output and x_0 is an initial value of the state vector (The MathWorks Inc., 2023d).

Appendix H

Figure. Load curve for large disturbance tests and minimum generator power definition.

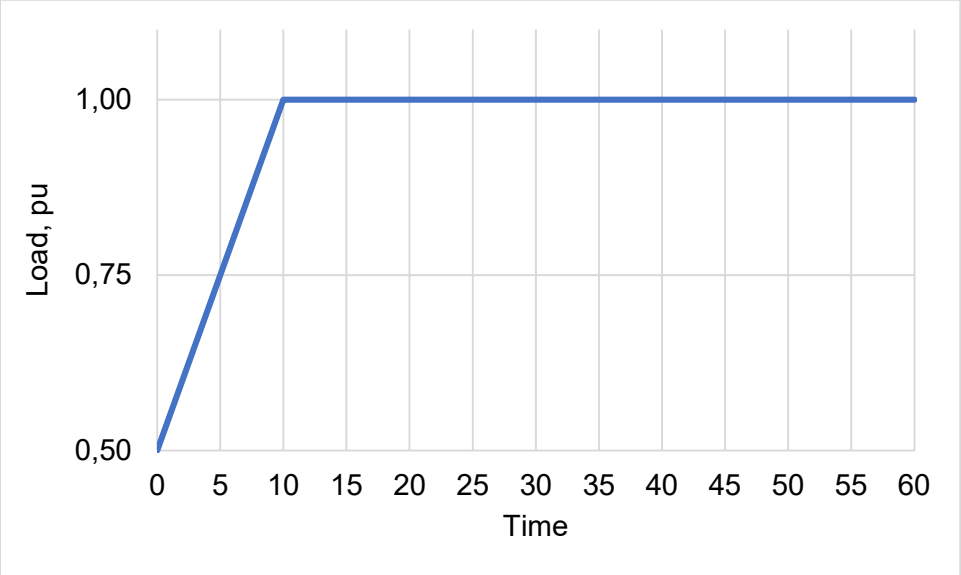

Figure. Voltage fluctuations in the case with maximum wind power.

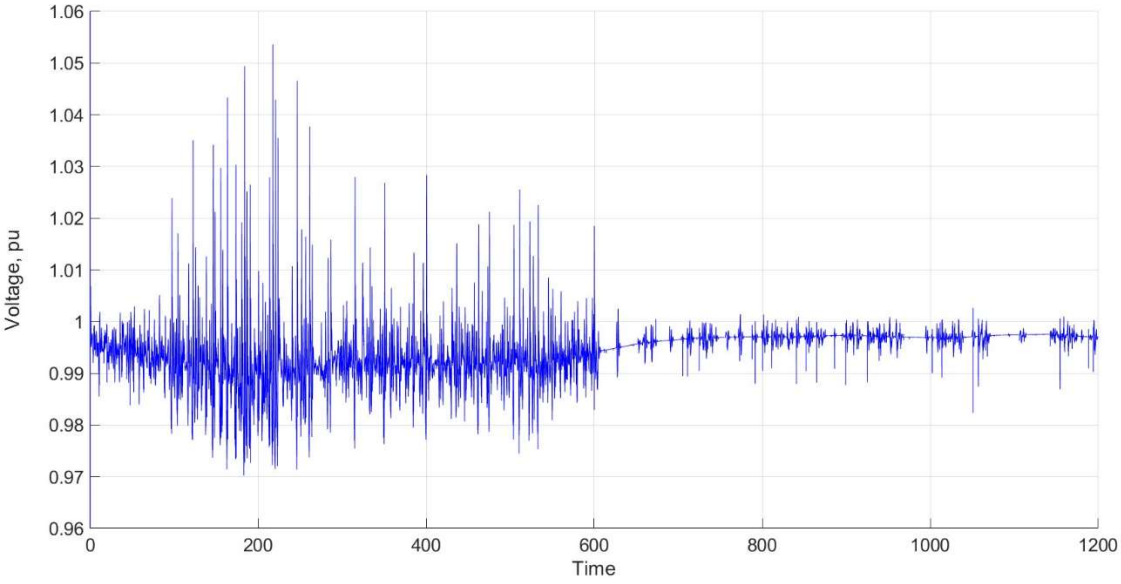

Figure. Load angle in the case with maximum wind power.

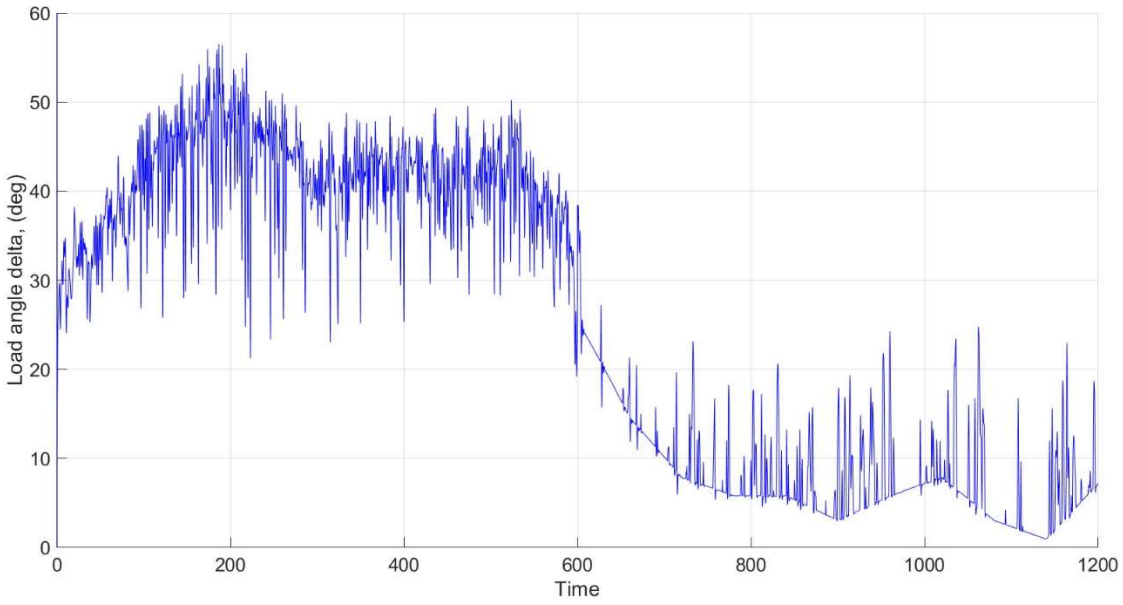

Figure. Load angle during transient stability tests in the case with maximum wind power.

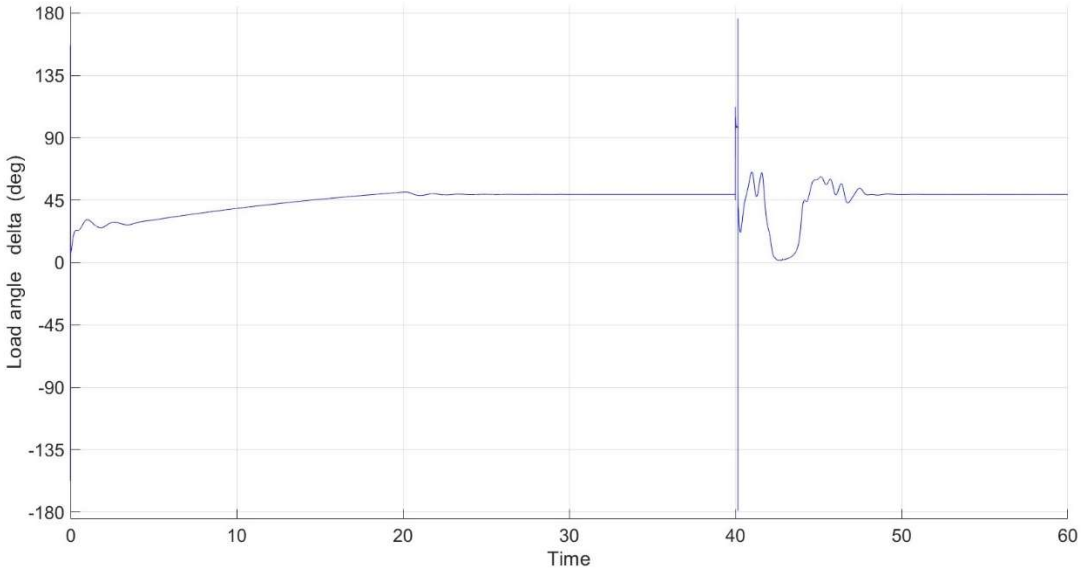

Figure. Large voltage disturbance on the generators line.

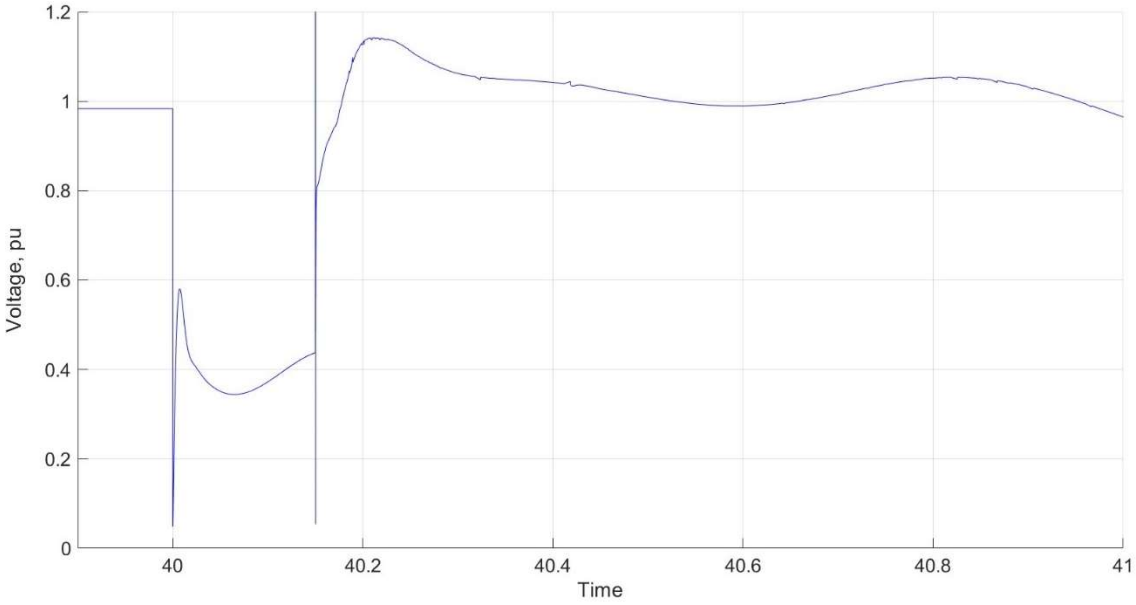

Figure. Large voltage disturbance on the turbine line.

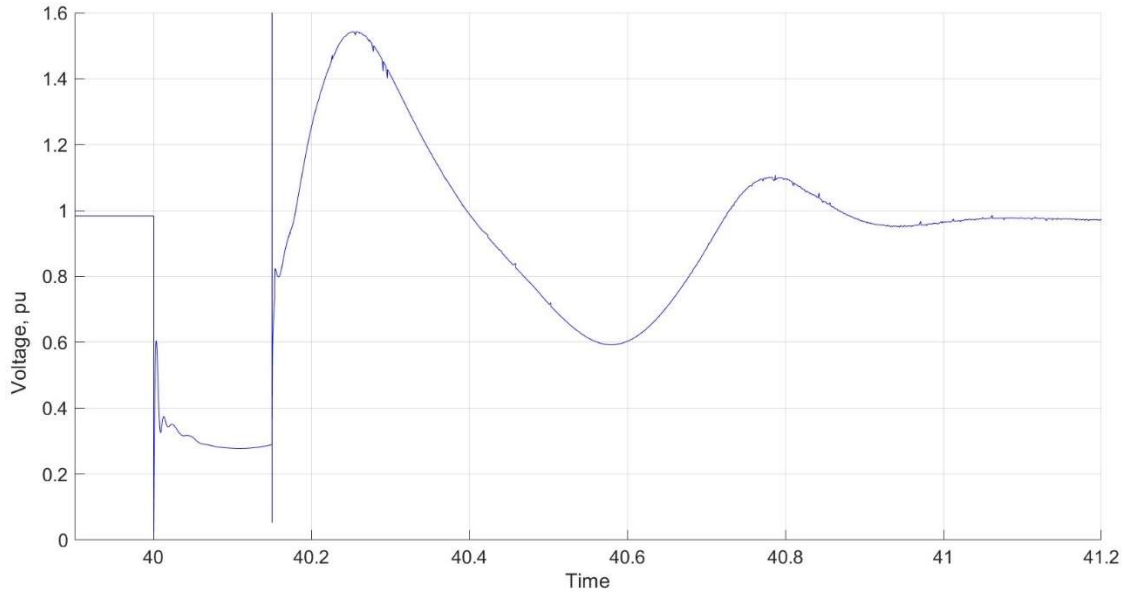

Appendix I

Table. 3-phase source block parameters.

Configuration	Internally grounded neutral
P-P voltage, kV (RMS)	33
Phase angle, degrees	0
Frequency, Hz	50
X/R ratio	10

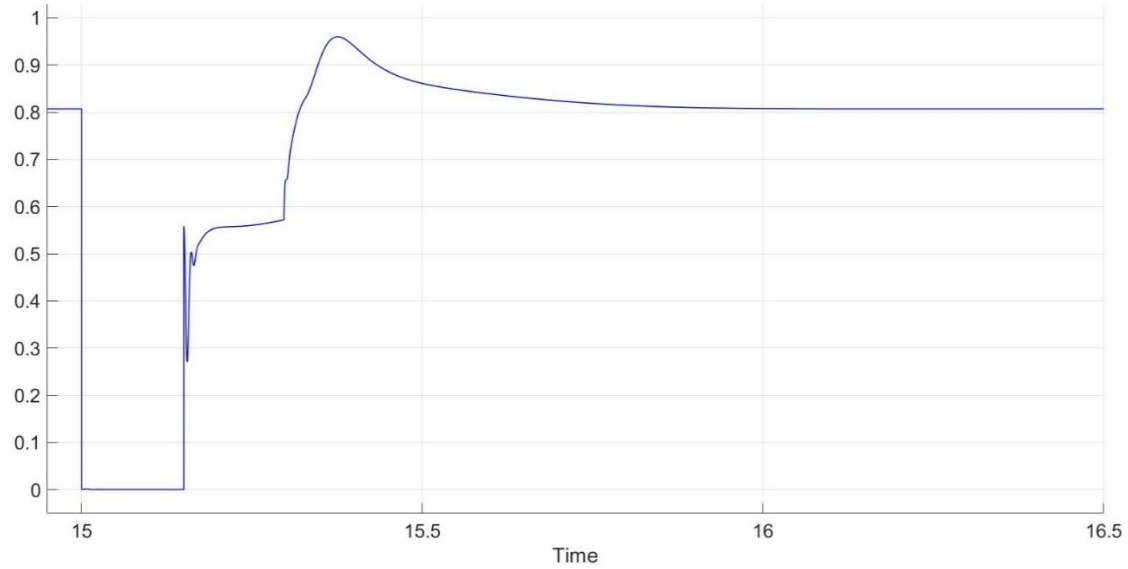

Figure. Fault test of 465 MW wind turbine capacity.

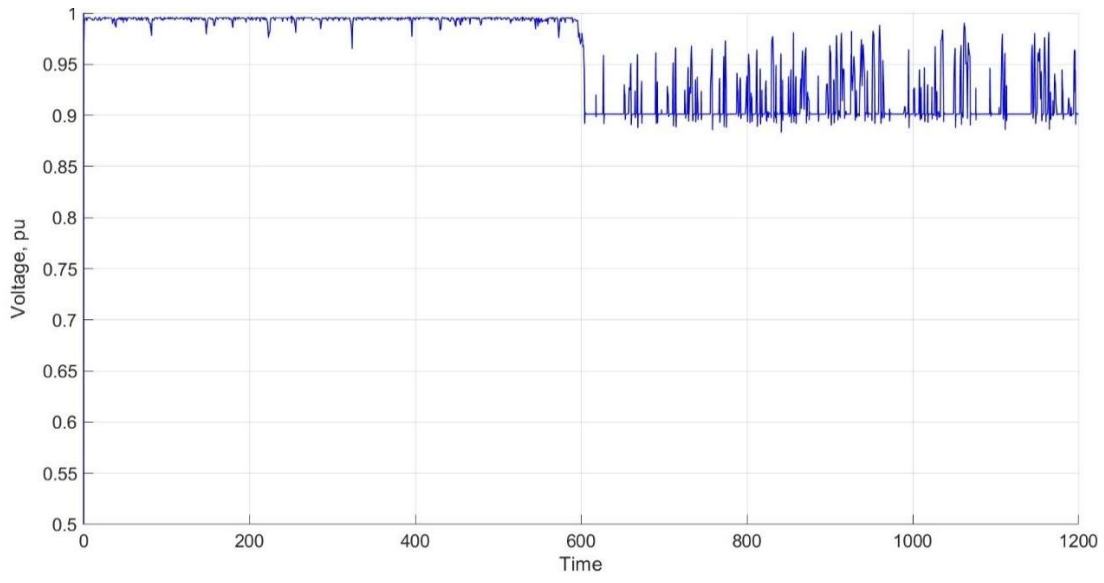

Figure. Voltage during wind fluctuations at PCC of 381,9 MW wind turbine capacity.